

Analytic Formulae for Inflationary Correlators with Dynamical Mass

Shuntaro Aoki ^{1*}, Toshifumi Noumi ^{2†}, Fumiya Sano ^{3,4‡},
Masahide Yamaguchi ^{4,3§}

¹*Particle Theory and Cosmology Group, Center for Theoretical Physics of the Universe,
Institute for Basic Science, Daejeon, 34126, Korea*

²*Graduate School of Arts and Sciences, The University of Tokyo, Tokyo 153-8902, Japan*

³*Department of Physics, Tokyo Institute of Technology, Tokyo 152-8551, Japan*

⁴*Cosmology, Gravity and Astroparticle Physics Group, Center for Theoretical Physics of the
Universe, Institute for Basic Science, Daejeon 34126, Korea*

Abstract

Massive fields can imprint unique oscillatory features on primordial correlation functions or inflationary correlators, which is dubbed the cosmological collider signal. In this work, we analytically investigate the effects of a *time-dependent* mass of a scalar field on inflationary correlators, extending previous numerical studies and implementing techniques developed in the cosmological bootstrap program. The time-dependent mass is in general induced by couplings to the slow-roll inflaton background, with particularly significant effects in the case of non-derivative couplings. By linearly approximating the time dependence, the mode function of the massive scalar is computed analytically, on which we derive analytic formulae for two-, three-, and four-point correlators with the tree-level exchange of the massive scalar. The obtained formulae are utilized to discuss the phenomenological impacts on the power spectrum and bispectrum, and it is found that the scaling behavior of the bispectrum in the squeezed configuration, i.e., the cosmological collider signal, is modified from a time-dependent Boltzmann suppression. By investigating the scaling behavior in detail, we are in principle able to determine the non-derivative couplings between the inflaton and the massive particle.

*E-mail address: shuntaro1230@gmail.com

†E-mail address: tnoumi@g.ecc.u-tokyo.ac.jp

‡E-mail address: sanof.cosmo@gmail.com

§E-mail address: gucci@ibs.re.kr

Contents

1	Introduction	1
2	Setup	3
2.1	Mode functions and propagators with time-dependent mass	3
2.2	Inflationary correlators	6
3	Bootstrapping Seed Integrals with Time-dependent Mass	10
3.1	Bootstrap equations	10
3.2	Solutions	13
3.3	Soft limit	17
4	Impact on Primordial non-Gaussianity	19
4.1	Power spectrum	20
4.2	Bispectrum	22
4.2.1	Cosmological collider signal at squeezed configuration	22
4.2.2	Distinction of couplings with inflaton	23
4.2.3	Equilateral configuration	25
5	Summary	26
A	Seed integral with the Mellin–Barnes representation	27
B	Constant Mass Limit	32
	References	33

1 Introduction

Observations of the Cosmic Microwave Background [1–3] strongly support the existence of cosmic inflation [4–8] which can give solutions to several problems in the standard cosmology as well as is the source of primordial scalar (curvature) and tensor perturbations. Furthermore, given the high energy scale ($\rho_{\text{inf}}^{1/4} \sim 10^{15}$ GeV at most), inflation is a unique opportunity to explore high energy physics including models beyond the Standard Model.

In recent year, there has been a growing interest in an approach that exploit higher-point correlation functions, or non-Gaussianity, of scalar and tensor perturbations, called cosmological collider (CC) program (see earlier works [9–12] and recent developments [13–100]). Indeed, these correlation functions can contain information of (possibly new) massive particles created during inflation, and especially in the soft limits, we expect a sharp oscillatory

behavior (what we call “signal”) characterized by the mass of particles around the Hubble scale.

A number of recent developments have been seen in the computational methods of primordial correlators. In particular, the so-called cosmological bootstrap method [101–138] (see also AdS techniques [139–144]) has made it possible to compute the correlation functions rigorously and analytically without having to perform the awkward time integrals of special functions in the cosmological in-in calculations (see Ref. [145, 146] for the detail). This allows us to evaluate not only the signal parts of CC but also the non-oscillatory parts (background). This is quite important to understand how large the net signal is.

So far, most of the studies have focused on situations where the masses of massive fields are constant, and consequently, the correlation function has a scale-invariant form. However, interactions with inflaton can produce a non-negligible time dependence on the masses of these massive fields, resulting in a scale-dependent correlation function. For example in Ref. [86], it is numerically shown that a significant deviation from the standard CC signal in bispectrum can be obtained in case of the non-derivative coupling $e^{\alpha\phi/M_{\text{Pl}}}\sigma^2$, where ϕ is an inflaton and σ is an isocurvature.

In this paper, we derive *analytic* formulae for two-, three-, and four-point inflaton correlation functions or “inflationary correlators”. We focus on a simple model consisting of an inflaton and a massive scalar field, where the inflaton imparts a time dependence on the massive scalar through interactions. We then solve the so-called “bootstrap equations” for the correlators [101] by approximating the time-dependence of the mass at the linear order of time. In the constant mass limit, our results consistently reproduce those obtained in Refs. [128, 132]. The analytic formulae allow us to take into account arbitrary momentum configurations and background parts, so that we can extract various phenomenological aspects of non-Gaussianity in a more precise manner. Specifically, the bispectrum (three-point correlation function of the curvature perturbation) in the squeezed limit contains information on the time dependence of the mass of σ , which is useful to distinguish couplings between inflaton and the massive field.

The paper is organized as follows. In section 2, we introduce the above setup and solve the mode equations for a massive scalar field with time-dependent mass. We also introduce integral formulae for the two-, three-, and four-point correlators of interest. We then derive and solve the bootstrap equations satisfied by the correlators in section 3. In section 4, we discuss the observational impact by taking a particular interaction between the inflaton and the massive scalar. Section 5 is devoted to the summary. Appendices A and B provide boundary conditions necessary to solve the bootstrap equations, and a consistency check in the constant mass limit.

Notations

The spacetime metric is Friedman–Lemaître–Robertson–Walker (FLRW) metric: $ds^2 = -dt^2 + a^2(t)d\mathbf{x}^2 = a^2(\tau)(-d\tau^2 + d\mathbf{x}^2)$, where t and τ are physical time and conformal

time respectively. In (quasi) de Sitter space, a scale factor is given by $a(\tau) = -1/H\tau$ with the Hubble parameter H . Regarding the derivative with respect to physical time (conformal time), we use a dot (prime) for operation, i.e., $\cdot = d/dt$ and $\prime = d/d\tau$.

2 Setup

In this work, we consider a simple system consisting of only an inflaton ϕ and a massive scalar σ , and assume that their interactions include the following non-derivative coupling:¹

$$\mathcal{L}_{\text{int}} \supset -\frac{1}{2}g(\phi)\sigma^2. \quad (2.1)$$

During inflation, the interaction (2.1) gives an effective mass of σ , $m_{\text{eff}}^2 = g(\phi_0(t))$ with $\phi_0(t)$ being the inflaton background, and thus the mass of σ becomes time-dependent. We will first investigate the effects of time dependence with Eq. (2.1) on the mode function of σ . Then, based on the mode function derived there, we study its impact on the inflationary correlation functions in the next sections.

2.1 Mode functions and propagators with time-dependent mass

Canonical quantization

We quantize the inflaton fluctuation $\delta\phi$ and the massive scalar σ with the mode expansion

$$\delta\phi(\tau, \mathbf{x}) = \int \frac{d^3\mathbf{k}}{(2\pi)^3} \left(u_k(\tau)a_{\mathbf{k}} + u_k^*(\tau)a_{-\mathbf{k}}^\dagger \right) e^{i\mathbf{k}\cdot\mathbf{x}}, \quad (2.2)$$

$$\sigma(\tau, \mathbf{x}) = \int \frac{d^3\mathbf{k}}{(2\pi)^3} \left(v_k(\tau)b_{\mathbf{k}} + v_k^*(\tau)b_{-\mathbf{k}}^\dagger \right) e^{i\mathbf{k}\cdot\mathbf{x}}, \quad (2.3)$$

and the commutation relations for the annihilation and the creation operators

$$[a_{\mathbf{k}}, a_{\mathbf{k}'}^\dagger] = (2\pi)^3 \delta^3(\mathbf{k} - \mathbf{k}'), \quad [b_{\mathbf{k}}, b_{\mathbf{k}'}^\dagger] = (2\pi)^3 \delta^3(\mathbf{k} - \mathbf{k}'). \quad (2.4)$$

Note that \mathbf{k} expresses three-dimensional vectors, and $k \equiv |\mathbf{k}|$ is the absolute value. Under the slow-roll approximation, the mode function of inflaton fluctuations, u_k , satisfies an equation of motion for a massless scalar field in de Sitter spacetime,

$$u_k'' - \frac{2}{\tau}u_k' + k^2 u_k = 0. \quad (2.5)$$

¹In this work, we do not consider back-reaction effects on the inflation dynamics due to Eq. (2.1), to keep our setup as simple as possible. But we only remark that these kinds of terms breaking a shift symmetry of inflaton affects the inflation dynamics in general at the classical and quantum level, which requires some non-trivial extension of the setup. For example, to relax the quantum effects, one may consider supersymmetric embedding [147] or a system with a discrete symmetry [148–150].

Assuming the Bunch–Davies vacuum, we obtain the canonically normalized mode function

$$u_k = \frac{H}{\sqrt{2k^3}}(1 + ik\tau)e^{-ik\tau}. \quad (2.6)$$

On the other hand, the mode function of the massive field, v_k , satisfies the following equation:

$$v_k'' - \frac{2}{\tau}v_k' + \left(k^2 + \frac{m_{\text{eff}}^2}{H^2\tau^2}\right)v_k = 0. \quad (2.7)$$

Here $m_{\text{eff}}^2 \equiv g(\phi_0(t))$ is an effective mass of σ , which in general depends on time.

Approximation of effective mass for analytic computations

In the forthcoming analysis, we impose several assumptions on the effective mass m_{eff} and employ approximations to perform analytic computations. To explain them, we begin by recalling that, within the framework of the slow-roll approximation, the inflaton background is described by

$$\phi_0(\tau) = \sqrt{2\epsilon}M_{\text{Pl}} \log\left(\frac{\tau}{\tau_0}\right), \quad (2.8)$$

where we used $\phi_0' = \sqrt{2\epsilon}M_{\text{Pl}}/\tau$ (assuming $\dot{\phi}_0 < 0$ without loss of generality) and introduced a reference time τ_0 as an integration constant. In this context, the value of the background inflaton field ϕ_{0*} at the horizon crossing time τ_* for a mode k is given by

$$\phi_{0*} = \sqrt{2\epsilon}M_{\text{Pl}} \log\left(\frac{\tau_*}{\tau_0}\right) = -\sqrt{2\epsilon}M_{\text{Pl}} \log v(k), \quad v(k) \equiv \frac{k}{k_0}, \quad (2.9)$$

where we used the condition $k\tau_* = -1$ and also introduced a reference scale k_0 such that $k_0\tau_0 = -1$. The effective mass at the horizon crossing of the mode k reads

$$m_{\text{eff}}^2(\tau_*) = g(\phi_{0*}) \equiv g_*(v). \quad (2.10)$$

We are interested in the situation where the variation of the effective mass is not negligible, i.e., $|\Delta m_{\text{eff}}^2| \gtrsim m_{\text{eff}}^2$ during observable inflation with e-folding number roughly $50 \lesssim N \lesssim 60$ for CMB, where Δm_{eff}^2 represents the change in the square of the effective mass from the beginning to the end of observable inflation. It is worth emphasizing that, under this condition, the time dependence of the effective mass produces significant effects that dominate over other slow-roll suppressed effects such as the inflaton mass. Moreover, we mainly focus on the situation that the effective mass remains at the Hubble scale throughout inflation, $m_{\text{eff}} \sim H$, and undergoes several times larger or smaller changes relative to the initial mass. This assumption is made to avoid exponential suppression of the CC signal $\sim e^{-\mathcal{O}(m_{\text{eff}}/H)}$.

When we solve the equation of motion (2.7) for the massive field σ , it is also necessary to consider the time evolution of the effective mass around the time of the horizon crossing.

In order to estimate the effect, let us perform an expansion of the inflaton background $\phi_0(\tau)$ around the horizon crossing time τ_* as

$$\phi_0(\tau) = \phi_{0*} - \sqrt{2\epsilon}M_{\text{Pl}} \left(1 - \frac{\tau}{\tau_*}\right) + \cdots, \quad (2.11)$$

where the dots stand for higher order terms in $1 - (\tau/\tau_*)$. Correspondingly, we expand the effective mass as

$$m_{\text{eff}}^2(\tau) = g_* - g_{\phi,*} \sqrt{2\epsilon}M_{\text{Pl}} \left(1 - \frac{\tau}{\tau_*}\right) + \cdots, \quad (2.12)$$

where $g_{\phi,*} \equiv dg/d\phi|_{\phi=\phi_{0*}}$. The expansion works well at least within a span of several e-foldings around the horizon crossing if the following condition is satisfied:

$$\frac{|g_{\phi,*}|M_{\text{Pl}}}{g_*} \lesssim \epsilon^{-1/2}. \quad (2.13)$$

In the following analysis, we will take into account the leading order correction, specifically, the second term of Eq. (2.12). On the other hand, the previously mentioned condition $|\Delta m_{\text{eff}}^2| \gtrsim m_{\text{eff}}^2$ for non-negligible time dependence during inflation can be rephrased as $|g_{\phi,*}|M_{\text{Pl}}/g_* \gtrsim \epsilon^{-1/2}\delta N^{-1}$ with $\delta N \sim 10$ being the change of the e-folding number over observable part of inflation and m_{eff}^2 being evaluated at the horizon crossing time. To sum up, there exists a parameter regime where both conditions are simultaneously satisfied:

$$\epsilon^{-1/2}\delta N^{-1} \lesssim \frac{|g_{\phi,*}|M_{\text{Pl}}}{g_*} \lesssim \epsilon^{-1/2}. \quad (2.14)$$

We work in this regime and study the effects of the time-dependent mass analytically.

Analytical mode function for massive field

With the leading order correction in Eq. (2.12), we simplify the equation of motion (2.7) for the massive field σ to

$$v_k'' - \frac{2}{\tau}v_k' + \left(k^2 + \frac{\mu^2 + 9/4}{\tau^2} + \frac{2k\kappa}{\tau}\right)v_k = 0 \quad (2.15)$$

where

$$\mu^2 \equiv \frac{g_*}{H^2} \left(1 - \frac{\sqrt{2\epsilon}g_{\phi,*}M_{\text{Pl}}}{g_*}\right) - \frac{9}{4}, \quad \kappa \equiv -\frac{g_*}{2H^2} \frac{\sqrt{2\epsilon}g_{\phi,*}M_{\text{Pl}}}{g_*}. \quad (2.16)$$

It is important to note that g_* and $g_{\phi,*}$ are functions of $v(k) = k/k_0$, thus μ and κ have scale dependence accordingly. We can solve Eq. (2.15) analytically as

$$v_k = \frac{e^{\pi\kappa/2}}{\sqrt{2k}} H(-\tau) W_{-i\kappa, i\mu}(2ik\tau), \quad (2.17)$$

where $W_{a,b}(\cdot)$ is the Whittaker function.² Note that when the mass of σ is constant, $g(\phi) = m_0^2$ (and hence $\kappa = 0$), Eq. (2.17) is reduced to

$$v_k = e^{-\frac{\pi}{2}\mu + i\frac{\pi}{4}} \frac{\sqrt{\pi}}{2} H(-\tau)^{3/2} H_{i\mu}^{(1)}(-k\tau) \quad (2.18)$$

with $\mu = \sqrt{(m_0/H)^2 - 9/4}$, which reproduces the mode function for a constant mass [9].

Propagators

Based on the mode functions, (2.6) and (2.17), one can construct Schwinger–Keldysh (SK) propagators as follows (see Ref. [146] for details).

- Bulk-to-boundary propagators for the inflaton fluctuation $\delta\phi$:

$$G_a(k; \tau) = \frac{H^2}{2k^3} (1 - ia k \tau) e^{iak\tau}, \quad (2.19)$$

where $a = \pm$.

- Bulk-to-bulk propagators D_{ab} with $a, b = \pm$ for the massive field σ :

$$D_{\pm\mp}(k; \tau_1, \tau_2) = D_{\leq}(k; \tau_1, \tau_2), \quad (2.20)$$

$$D_{\pm\pm}(k; \tau_1, \tau_2) = D_{\geq}(k; \tau_1, \tau_2) \theta(\tau_1 - \tau_2) + D_{\leq}(k; \tau_1, \tau_2) \theta(\tau_2 - \tau_1), \quad (2.21)$$

where $\theta(\cdot)$ is a unit step function and

$$D_{>}(k; \tau_1, \tau_2) = v_k(\tau_1) v_k^*(\tau_2) = \frac{e^{\pi\kappa}}{2k} H^2(\tau_1 \tau_2) W_{-i\kappa, i\mu}(2ik\tau_1) W_{i\kappa, -i\mu}(-2ik\tau_2), \quad (2.22)$$

$$D_{<}(k; \tau_1, \tau_2) = D_{>}^*(k; \tau_1, \tau_2). \quad (2.23)$$

2.2 Inflationary correlators

Here, we specify inflationary correlation functions to be investigated in this paper. The correlation functions can be computed from the formula [145],

$$\langle \mathcal{O} \rangle \equiv \langle 0 | \left[\bar{T} \exp \left(i \int_{-\infty}^0 d\tau' H_I(\tau') \right) \right] \mathcal{O}_I \left[T \exp \left(-i \int_{-\infty}^0 d\tau' H_I(\tau') \right) \right] | 0 \rangle, \quad (2.24)$$

where \mathcal{O} is the operator of our interest, and T (\bar{T}) is a (anti) time-ordering operator. H_I is an interaction Hamiltonian, and all quantities on the right-hand side are understood in the interaction picture.

²In this paper, we focus on the case with $\mu^2 > 0$ to see how the oscillatory features of the cosmological collider signal are affected by the time-dependent mass.

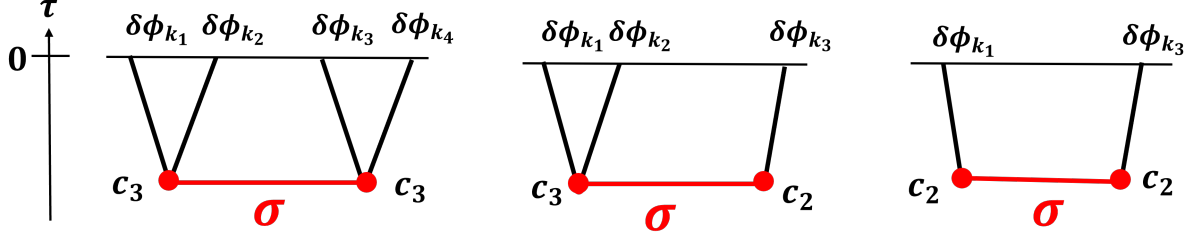


Figure 1 Diagrams with a massive scalar field σ with time-dependent mass.

Interactions

In addition to Eq. (2.1), we assume the presence of the following derivative (shift-symmetric with respect to $\delta\phi$) interactions involving the inflaton fluctuation $\delta\phi$ and the massive scalar σ ,

$$\mathcal{L}_{2,\text{int}} = c_2(-H\tau)^{-3}\sigma\delta\phi', \quad (2.25)$$

$$\mathcal{L}_{3,\text{int}} = c_3(-H\tau)^{-2}\sigma(\delta\phi')^2, \quad (2.26)$$

where c_2 and c_3 are coupling constants with mass dimension 1 and -1 , respectively. With the presence of the interactions and the formula (2.24), we can calculate inflationary correlators $\langle\delta\phi\cdots\delta\phi\rangle$. In particular, this paper focuses on analyzing the two-, three-, and four-point correlation functions of the inflaton fluctuations as shown in Fig. 1.

Before proceeding, let us comment on other types of ϕ - σ interactions which arise from the non-derivative coupling (2.1) and have unavoidable contribution to inflaton correlators. The interaction (2.1) can be expanded as

$$g(\phi)\sigma^2 = m_{\text{eff}}^2\sigma^2 + g_\phi\delta\phi\sigma^2 + \cdots, \quad (2.27)$$

and the second term, in conjunction with two transfer vertices (2.25), contributes to the three-point inflaton correlator as a tree, double σ -exchange diagram, in addition to the diagram of our interest (the middle diagram with single σ -exchange of Fig. 1). The contribution from the double-exchange diagram is estimated as

$$\langle\delta\phi^3\rangle_{\text{DE}} \sim g_\phi c_2^2, \quad (2.28)$$

while the one from the single-exchange diagram is

$$\langle\delta\phi^3\rangle_{\text{SE}} \sim H^3 c_2 c_3. \quad (2.29)$$

Here, in order to compare these contributions, let us further assume that the interactions, (2.25) and (2.26), are generated from a single covariant interaction $\sigma(\partial\phi)^2/\Lambda$ with a cutoff scale Λ . Then, the coupling constants are fixed as $c_2 \sim \sqrt{\epsilon}M_{\text{Pl}}H/\Lambda$ and $c_3 \sim 1/\Lambda$, and thus the ratio of these two correlators is evaluated as

$$\frac{1}{\delta N} \lesssim \frac{\langle\delta\phi^3\rangle_{\text{DE}}}{\langle\delta\phi^3\rangle_{\text{SE}}} \sim \frac{\sqrt{\epsilon}M_{\text{Pl}}g_\phi}{H^2} \lesssim 1. \quad (2.30)$$

The inequalities are from the lower and the upper bound of Eq. (2.14) with the quasi-single field regime $m_{\text{eff}}^2 = g(\phi_0) \sim H^2$. Therefore, we find the contribution from the double-exchange diagram is comparable to or smaller than the single-exchange one in the cosmological collider setup. In section 4 where some phenomenological aspects of the time-dependent mass are discussed, we choose the model parameters within the region (2.30), in particular near the lower bound. In this case, the contribution from the double-exchange is negligible (about 10% of the single-exchange contribution). Furthermore, each massive propagator is naively expected to be suppressed by the Boltzmann factor $e^{-\pi\mu}$, leading to the prediction that the double exchange process can receive stronger suppression by one more Boltzmann factor than the single-exchange process³. Taking the above discussions into account, we ignore the contribution from the double-exchange diagram in this work⁴.

4-point correlators

Let us begin with the correction to the four-point correlation functions since its specific limit produces the three- and two-point correlation functions.

By employing the in-in formula (2.24) (or SK diagrammatic rule [146]), we obtain

$$\begin{aligned} & \langle \delta\phi_{\mathbf{k}_1} \delta\phi_{\mathbf{k}_2} \delta\phi_{\mathbf{k}_3} \delta\phi_{\mathbf{k}_4} \rangle' \\ &= -4 \frac{c_3^2}{H^4} \sum_{a,b=\pm} ab \int \frac{d\tau_1}{(-\tau_1)^2} \frac{d\tau_2}{(-\tau_2)^2} G'_a(k_1; \tau_1) G'_a(k_2; \tau_1) G'_b(k_3; \tau_2) G'_b(k_4; \tau_2) D_{ab}(k_s; \tau_1, \tau_2) + 5\text{per.}, \end{aligned} \quad (2.31)$$

where the prime on the left-hand side means that a momentum conservation factor $(2\pi)^3 \delta^{(3)}(\mathbf{k}_1 + \dots + \mathbf{k}_4)$ is extracted, and “5 per.” represents permutations of the external momenta \mathbf{k}_i ($i = 1, \dots, 4$). The propagators G_a and D_{ab} are given in Eqs. (2.19), (2.20) and (2.21) respectively, and $k_s \equiv |\mathbf{k}_1 + \mathbf{k}_2|$ is the “ s -channel” momentum. This can be further simplified as

$$\begin{aligned} & \langle \delta\phi_{\mathbf{k}_1} \delta\phi_{\mathbf{k}_2} \delta\phi_{\mathbf{k}_3} \delta\phi_{\mathbf{k}_4} \rangle' \\ &= -4c_3^2 H^4 \cdot \frac{1}{16k_1 k_2 k_3 k_4} \sum_{a,b=\pm} ab \int d\tau_1 d\tau_2 e^{ia k_{12} \tau_1 + ib k_{34} \tau_2} D_{ab}(k_s; \tau_1, \tau_2) + 5\text{per.} \\ &= 4c_3^2 H^4 \cdot \frac{1}{16k_1 k_2 k_3 k_4 k_s^5} \sum_{a,b=\pm} \mathcal{I}_{ab}^{0,0} + 5\text{per.}, \end{aligned} \quad (2.32)$$

³Note that it was numerically shown that the triple-exchange diagram exhibits only a single Boltzmann suppression factor in Ref. [146], so we need more detailed analysis for double-exchange one.

⁴An analytic approach to multiple exchange diagrams was recently discussed in Ref. [135]. As in this work, it would be interesting to consider the effects of time-dependent couplings on these more general diagrams. We leave it as non-trivial future works.

where $k_{12} \equiv k_1 + k_2$ and $k_{34} \equiv k_3 + k_4$. In the first line we inserted the explicit expression of G_a , and in the second line we introduced a “seed integral” [128, 132],

$$\mathcal{I}_{ab}^{p_1 p_2} \equiv -ab k_s^{5+p_{12}} \int_{-\infty}^0 d\tau_1 d\tau_2 (-\tau_1)^{p_1} (-\tau_2)^{p_2} e^{iak_{12}\tau_1 + ibk_{34}\tau_2} D_{ab}(k_s; \tau_1, \tau_2), \quad (2.33)$$

with p_1 and p_2 being constant numbers with $p_{1,2} > -5/2$, and $p_{12} \equiv p_1 + p_2$. Therefore, once the seed integral (2.33) is computed, the four-point correlation function can be automatically obtained from Eq. (2.32), and this is also true for three- and two-point functions, as shown below.

3-point correlators

In the same way, by utilizing the seed integral (2.33), the three-point function is given by

$$\begin{aligned} & \langle \delta\phi_{\mathbf{k}_1} \delta\phi_{\mathbf{k}_2} \delta\phi_{\mathbf{k}_3} \rangle' \\ &= -2 \frac{c_2 c_3}{H^5} \sum_{a,b=\pm} ab \int \frac{d\tau_1}{(-\tau_1)^2} \frac{d\tau_2}{(-\tau_2)^3} G'_a(k_1; \tau_1) G'_a(k_2; \tau_1) G'_b(k_3; \tau_2) D_{ab}(k_3; \tau_1, \tau_2) + 2\text{per.} \\ &= 2c_2 c_3 H \cdot \frac{1}{8k_1 k_2 k_3} \sum_{a,b=\pm} ab \int d\tau_1 \frac{d\tau_2}{(-\tau_2)^2} e^{iak_{12}\tau_1 + ibk_{34}\tau_2} D_{ab}(k_3; \tau_1, \tau_2) + 2\text{per.} \\ &= -2c_2 c_3 H \cdot \frac{1}{8k_1 k_2 k_3^4} \lim_{k_4 \rightarrow 0} \sum_{a,b=\pm} \mathcal{I}_{ab}^{0,-2} + 2\text{per.} \end{aligned} \quad (2.34)$$

The three-point correlator corresponds to a soft limit ($k_4 \rightarrow 0$) of the four-point one or the seed integral.

2-point correlators

Finally, the leading order correction to the two-point function is described as follows:

$$\begin{aligned} \langle \delta\phi_{\mathbf{k}_1} \delta\phi_{\mathbf{k}_3} \rangle' &= -\frac{c_2^2}{H^6} \sum_{a,b=\pm} ab \int \frac{d\tau_1}{(-\tau_1)^3} \frac{d\tau_2}{(-\tau_2)^3} G'_a(k_1; \tau_1) G'_b(k_1; \tau_2) D_{ab}(k_1; \tau_1, \tau_2) \\ &= -\frac{c_2^2}{H^2} \cdot \frac{1}{4k_1^2} \sum_{a,b=\pm} ab \int \frac{d\tau_1}{(-\tau_1)^2} \frac{d\tau_2}{(-\tau_2)^2} e^{iak_1\tau_1 + ibk_1\tau_2} D_{ab}(k_1; \tau_1, \tau_2) \\ &= \frac{c_2^2}{H^2} \cdot \frac{1}{4k_1^3} \lim_{k_2, k_4 \rightarrow 0} \sum_{a,b=\pm} \mathcal{I}_{ab}^{-2,-2}. \end{aligned} \quad (2.35)$$

Here, we need an expression for double soft limits ($k_2, k_4 \rightarrow 0$) of the seed integral. Note that the above correlator is a correction to the one in free theory, $\langle \delta\phi_{\mathbf{k}_1} \delta\phi_{\mathbf{k}_3} \rangle' = H^2/2k_1^3$.

3 Bootstrapping Seed Integrals with Time-dependent Mass

Our task is reduced to evaluate the seed integral (2.33),

$$\mathcal{I}_{\text{ab}}^{p_1 p_2} \equiv -\text{ab} k_s^{5+p_{12}} \int_{-\infty}^0 d\tau_1 d\tau_2 (-\tau_1)^{p_1} (-\tau_2)^{p_2} e^{i\text{a}k_{12}\tau_1 + i\text{b}k_{34}\tau_2} D_{\text{ab}}(k_s; \tau_1, \tau_2). \quad (3.1)$$

Performing the time-integral in Eq. (3.1) is challenging for general momentum configurations. Therefore, we employ another approach developed in Refs. [101, 128, 132], where we can obtain analytic expressions for the seed integrals by solving differential equations (“bootstrap equations”) for Eq. (3.1). We will see that this method is also applicable to our case. Note that this section describes technical details, so readers who are not interested in the derivation can skip to the final results, Eqs. (3.47), (3.48) for the seed integral, Eqs. (3.53), (3.54) for its single soft limit, and Eqs. (3.59), (3.60) for the double soft limit.

3.1 Bootstrap equations

The SK propagators in Eqs. (2.20) and (2.21) satisfy the following differential equations

$$\left(\tau_1^2 \partial_{\tau_1}^2 - 2\tau_1 \partial_{\tau_1} + k_s^2 \tau_1^2 + \mu^2 + \frac{9}{4} + 2\kappa k_s \tau_1 \right) D_{\pm\mp}(k_s; \tau_1, \tau_2) = 0, \quad (3.2)$$

$$\left(\tau_1^2 \partial_{\tau_1}^2 - 2\tau_1 \partial_{\tau_1} + k_s^2 \tau_1^2 + \mu^2 + \frac{9}{4} + 2\kappa k_s \tau_1 \right) D_{\pm\pm}(k_s; \tau_1, \tau_2) = \mp i H^2 \tau_1^2 \tau_2^2 \delta(\tau_1 - \tau_2), \quad (3.3)$$

where we recall $k_s \equiv |\mathbf{k}_1 + \mathbf{k}_2|$. They satisfy the same differential equations with respect to τ_2 . By introducing

$$z_1 = -k_{12}\tau_1, \quad z_2 = -k_{34}\tau_2, \quad (3.4)$$

with $k_{12} \equiv k_1 + k_2$ and $k_{34} \equiv k_3 + k_4$, and

$$r_1 \equiv \frac{k_s}{k_{12}}, \quad r_2 \equiv \frac{k_s}{k_{34}}, \quad (3.5)$$

Eqs. (3.2) and (3.3) can be rewritten as

$$\left(z_1^2 \partial_{z_1}^2 - 2z_1 \partial_{z_1} + r_1^2 z_1^2 + \mu^2 + \frac{9}{4} - 2\kappa r_1 z_1 \right) \widehat{D}_{\pm\mp}(r_1 z_1, r_2 z_2) = 0, \quad (3.6)$$

$$\left(z_1^2 \partial_{z_1}^2 - 2z_1 \partial_{z_1} + r_1^2 z_1^2 + \mu^2 + \frac{9}{4} - 2\kappa r_1 z_1 \right) \widehat{D}_{\pm\pm}(r_1 z_1, r_2 z_2) = \mp i H^2 r_1^2 z_1^2 r_2^2 z_2^2 \delta(r_1 z_1 - r_2 z_2), \quad (3.7)$$

where we defined $\widehat{D}_{ab} = k_s^3 D_{ab}$, or explicitly,

$$\widehat{D}_{\pm\mp}(r_1 z_1, r_2 z_2) = \frac{e^{\pi\kappa}}{2} H^2 r_1 z_1 r_2 z_2 W_{\pm i\kappa, \mp i\mu}(\pm 2i r_1 z_1) W_{\mp i\kappa, \pm i\mu}(\mp 2i r_2 z_2), \quad (3.8)$$

$$\widehat{D}_{\pm\pm}(r_1 z_1, r_2 z_2) = \theta(r_2 z_2 - r_1 z_1) \widehat{D}_{\mp\pm}(r_1 z_1, r_2 z_2) + \theta(r_1 z_1 - r_2 z_2) \widehat{D}_{\pm\mp}(r_1 z_1, r_2 z_2). \quad (3.9)$$

An important observation is that \widehat{D} depends on z_i ($i = 1, 2$) with a specific combination $r_i z_i$. Thus, Eqs. (3.6) and (3.7) can be regarded as the differential equations with respect to r_i , i.e.,

$$\left(r_1^2 \partial_{r_1}^2 - 2r_1 \partial_{r_1} + r_1^2 z_1^2 + \mu^2 + \frac{9}{4} - 2\kappa r_1 z_1 \right) \widehat{D}_{\pm\mp}(r_1 z_1, r_2 z_2) = 0, \quad (3.10)$$

$$\left(r_1^2 \partial_{r_1}^2 - 2r_1 \partial_{r_1} + r_1^2 z_1^2 + \mu^2 + \frac{9}{4} - 2\kappa r_1 z_1 \right) \widehat{D}_{\pm\pm}(r_1 z_1, r_2 z_2) = \mp i H^2 r_1^2 z_1^2 r_2^2 z_2^2 \delta(r_1 z_1 - r_2 z_2), \quad (3.11)$$

and similarly for r_2 .

The subsequent task is identifying differential equations (bootstrap equations) for the seed integral. In terms of z_i and r_i , Eq. (3.1) is expressed as

$$\mathcal{I}_{ab}^{p_1 p_2} = (-ab) r_1^{1+p_1} r_2^{1+p_2} \int_0^\infty dz_1 dz_2 z_1^{p_1} z_2^{p_2} e^{-ia z_1 - ib z_2} \widehat{D}_{ab}(r_1 z_1, r_2 z_2). \quad (3.12)$$

Let us start from the opposite sign seed integral $\mathcal{I}_{\pm\mp}^{p_1 p_2}$. By applying Eq. (3.10), $r_1^{-1-p_1} r_2^{-1-p_2} \mathcal{I}_{\pm\mp}^{p_1 p_2}$ satisfies

$$\begin{aligned} & \left(r_1^2 \partial_{r_1}^2 - 2r_1 \partial_{r_1} + \mu^2 + \frac{9}{4} \right) \left(r_1^{-1-p_1} r_2^{-1-p_2} \mathcal{I}_{\pm\mp}^{p_1 p_2} \right) \\ &= \int_0^\infty dz_1 dz_2 z_1^{p_1} z_2^{p_2} e^{\mp i z_1 \pm i z_2} \left(r_1^2 \partial_{r_1}^2 - 2r_1 \partial_{r_1} + \mu^2 + \frac{9}{4} \right) \widehat{D}_{\pm\mp}(r_1 z_1, r_2 z_2) \\ &= \int_0^\infty dz_1 dz_2 z_1^{p_1} z_2^{p_2} e^{\mp i z_1 \pm i z_2} \left(-r_1^2 z_1^2 + 2\kappa r_1 z_1 \right) \widehat{D}_{\pm\mp}(r_1 z_1, r_2 z_2) \\ &= \left[r_1^2 (r_1 \partial_{r_1} + p_1 + 2) (r_1 \partial_{r_1} + p_1 + 1) \mp 2i\kappa r_1 (r_1 \partial_{r_1} + p_1 + 1) \right] \left(r_1^{-1-p_1} r_2^{-1-p_2} \mathcal{I}_{\pm\mp}^{p_1 p_2} \right), \end{aligned} \quad (3.13)$$

where we used the following formulae for an arbitrary function $f(rz)$,

$$\int_0^\infty dz z^{p+1} e^{-iaz} f(rz) = -ia(r\partial_r + p + 1) \int_0^\infty dz z^p e^{-iaz} f(rz), \quad (3.14)$$

$$\int_0^\infty dz z^{p+2} e^{-iaz} f(rz) = -(r\partial_r + p + 2)(r\partial_r + p + 1) \int_0^\infty dz z^p e^{-iaz} f(rz), \quad (3.15)$$

from the third to the fourth line. Thus, we find

$$\begin{aligned} & \left[\left(r_1^2 - r_1^4 \right) \partial_{r_1}^2 - 2 \left(r_1 + (p_1 + 2) r_1^3 \mp i\kappa r_1^2 \right) \partial_{r_1} + \left(\mu^2 + \frac{9}{4} - (p_1 + 1)(p_1 + 2) r_1^2 \pm 2(p_1 + 1)i\kappa r_1 \right) \right] \\ & \times \left(r_1^{-1-p_1} r_2^{-1-p_2} \mathcal{I}_{\pm\mp}^{p_1 p_2} \right) = 0, \end{aligned} \quad (3.16)$$

or equivalently,

$$\mathcal{D}_{\pm, r_1}^{p_1} \mathcal{I}_{\pm\mp}^{p_1 p_2} = 0, \quad (3.17)$$

where

$$\mathcal{D}_{\pm, r}^p \equiv (r^2 - r^4) \partial_r^2 - 2 \left[(p+2)r + r^3 \mp i\kappa r^2 \right] \partial_r + \mu^2 + \frac{(5+2p)^2}{4}. \quad (3.18)$$

Eq. (3.17) gives the bootstrap equations for $\mathcal{I}_{\pm\mp}^{p_1 p_2}$ with respect to r_1 . Those with respect to r_2 are obtained in the same way, $\mathcal{D}_{\mp, r_2}^{p_1} \mathcal{I}_{\pm\mp}^{p_1 p_2} = 0$.

Let us shift our focus to the seed integral with the same sign, $\mathcal{I}_{\pm\pm}^{p_1 p_2}$. The derivation is basically parallel to the previous case, except for the presence of the “source” term on the right-hand side of Eq. (3.7). In fact, we find

$$\begin{aligned} & \left(r_1^2 \partial_{r_1}^2 - 2r_1 \partial_{r_1} + \mu^2 + \frac{9}{4} \right) \left(r_1^{-1-p_1} r_2^{-1-p_2} \mathcal{I}_{\pm\pm}^{p_1 p_2} \right) \\ &= \left[r_1^2 (r_1 \partial_{r_1} + p_1 + 2) (r_1 \partial_{r_1} + p_1 + 1) \mp 2i\kappa r_1 (r_1 \partial_{r_1} + p_1 + 1) \right] \left(r_1^{-1-p_1} r_2^{-1-p_2} \mathcal{I}_{\pm\pm}^{p_1 p_2} \right) \\ & \quad \pm iH^2 r_1^2 r_2^2 \int_0^\infty dz_1 dz_2 z_1^{p_1+2} z_2^{p_2+2} e^{\mp i z_1 \mp i z_2} \delta(r_1 z_1 - r_2 z_2), \end{aligned} \quad (3.19)$$

where the second term of the right-hand side is the new contribution. After performing the one-dimensional integral, we obtain the bootstrap equations

$$\mathcal{D}_{\pm, r_1}^{p_1} \mathcal{I}_{\pm\pm}^{p_1 p_2} = H^2 e^{\mp i p_{12} \frac{\pi}{2}} \Gamma(5 + p_{12}) \left(\frac{r_1 r_2}{r_1 + r_2} \right)^{5+p_{12}}. \quad (3.20)$$

The same equation for r_2 is provided with a replacement $\mathcal{D}_{\pm, r_1}^{p_1} \rightarrow \mathcal{D}_{\pm, r_2}^{p_1}$.

As pointed out in Refs. [128, 132], it is useful to introduce new variables

$$u_i \equiv \frac{2r_i}{1 + r_i}, \quad (i = 1, 2). \quad (3.21)$$

In terms of u_i , the set of bootstrap equations is summarized as

$$\mathcal{D}_{\pm, u_1}^{p_1} \mathcal{I}_{\pm\mp}^{p_1 p_2} = 0, \quad (3.22)$$

$$\mathcal{D}_{\pm, u_1}^{p_1} \mathcal{I}_{\pm\pm}^{p_1 p_2} = H^2 e^{\mp i p_{12} \frac{\pi}{2}} \Gamma(5 + p_{12}) \left(\frac{u_1 u_2}{2(u_1 + u_2 - u_1 u_2)} \right)^{5+p_{12}}, \quad (3.23)$$

and

$$\mathcal{D}_{\mp, u_2}^{p_2} \mathcal{I}_{\pm\mp}^{p_1 p_2} = 0, \quad (3.24)$$

$$\mathcal{D}_{\pm, u_2}^{p_2} \mathcal{I}_{\pm\pm}^{p_1 p_2} = H^2 e^{\mp i p_{12} \frac{\pi}{2}} \Gamma(5 + p_{12}) \left(\frac{u_1 u_2}{2(u_1 + u_2 - u_1 u_2)} \right)^{5+p_{12}}, \quad (3.25)$$

where

$$\mathcal{D}_{\pm, u}^p \equiv (u^2 - u^3) \partial_u^2 - \left[(4 + 2p)u - (1 + p \pm i\kappa)u^2 \right] \partial_u + \left[\mu^2 + \left(p + \frac{5}{2} \right)^2 \right]. \quad (3.26)$$

3.2 Solutions

Here we solve the bootstrap equations, (3.22), (3.23), (3.24), and (3.25).

Opposite sign seed $\mathcal{I}_{\pm\mp}^{p_1 p_2}$

The opposite sign seeds $\mathcal{I}_{\pm\mp}^{p_1 p_2}$ satisfy the homogeneous differential equations, (3.22) and (3.24). Considering each equation has two independent solutions, a general solution for $\mathcal{I}_{\pm\mp}^{p_1 p_2}$ can be expressed as the following combination:

$$\mathcal{I}_{\pm\mp}^{p_1 p_2} = \sum_{a,b=\pm} \mathcal{C}_{\pm\mp|ab} \mathcal{U}_{\pm|a}^{p_1}(u_1) \mathcal{U}_{\mp|b}^{p_2}(u_2), \quad (3.27)$$

where $\mathcal{C}_{\pm\mp|ab}$ are coefficients fixed from boundary conditions later, and $\mathcal{U}_{a|b}(u)$ with $b = \pm 1$ are the two independent solutions

$$\mathcal{U}_{a|b}^p(u) = iab 2^{iab\mu} \pi \operatorname{csch}(2\pi\mu) \left(\frac{u}{2}\right)^{5/2+p+iab\mu} {}_2\mathcal{F}_1 \left[\begin{matrix} \frac{5}{2} + p + iab\mu, \frac{1}{2} - ia\kappa + iab\mu \\ 1 + 2iab\mu \end{matrix} \middle| u \right]. \quad (3.28)$$

Here, we inserted some numerical factors for later convenience, and ${}_p\mathcal{F}_q$ is defined by

$${}_p\mathcal{F}_q \left[\begin{matrix} a_1, \dots, a_p \\ b_1, \dots, b_q \end{matrix} \middle| z \right] \equiv \Gamma \left[\begin{matrix} a_1, \dots, a_p \\ b_1, \dots, b_q \end{matrix} \right] {}_pF_q \left[\begin{matrix} a_1, \dots, a_p \\ b_1, \dots, b_q \end{matrix} \middle| z \right], \quad (3.29)$$

where ${}_pF_q$ is a generalized hypergeometric function, and the products of gamma function is abbreviated by

$$\Gamma[z_1, \dots, z_m] \equiv \Gamma(z_1) \cdots \Gamma(z_m), \quad (3.30)$$

$$\Gamma \left[\begin{matrix} z_1, \dots, z_m \\ w_1, \dots, w_n \end{matrix} \right] \equiv \frac{\Gamma(z_1) \cdots \Gamma(z_m)}{\Gamma(w_1) \cdots \Gamma(w_n)}. \quad (3.31)$$

Same sign seed $\mathcal{I}_{\pm\pm}^{p_1 p_2}$

The same sign seeds $\mathcal{I}_{\pm\pm}^{p_1 p_2}$ satisfy the inhomogeneous differential equations, (3.23) and (3.25). The general solution is obtained by combining the general solution for the corresponding homogeneous equation with the particular solution for the inhomogeneous one. Therefore, we can take

$$\mathcal{I}_{\pm\pm}^{p_1 p_2} = \mathcal{G}_{\pm\pm}^{p_1 p_2} + \sum_{a,b=\pm} \mathcal{C}_{\pm\pm|ab} \mathcal{U}_{\pm|a}^{p_1}(u_1) \mathcal{U}_{\pm|b}^{p_2}(u_2), \quad (3.32)$$

where $\mathcal{G}_{\pm\pm}^{p_1 p_2}$ is a particular solution and the second term is the solution for homogeneous equations consisting of undetermined coefficients $\mathcal{C}_{\pm\pm|ab}$ and Eq. (3.28).

Regarding the particular solution, we rewrite the right-hand side of Eq. (3.23) by using

$$\left(\frac{u_1 u_2}{2(u_1 + u_2 - u_1 u_2)}\right)^{5+p_{12}} = \left(\frac{u_1}{2}\right)^{p_{12}+5} \sum_{n=0}^{\infty} \binom{n+p_{12}+4}{n} u_1^n \left(1 - \frac{1}{u_2}\right)^n, \quad (3.33)$$

where the array on the right-hand side means the binomial coefficient. This motivates us to take the following ansatz for $\mathcal{G}_{\pm\pm}^{p_1 p_2}$:

$$\mathcal{G}_{\pm\pm}^{p_1 p_2} = \frac{H^2 e^{\mp \frac{\pi}{2} i p_{12}} \Gamma(p_{12} + 5)}{2^{p_{12}+5}} \sum_{m,n=0}^{\infty} \chi_{m,n}^{\pm} u_1^{m+n+p_{12}+5} \left(1 - \frac{1}{u_2}\right)^n. \quad (3.34)$$

Inserting Eqs. (3.33) and (3.34) to Eq. (3.23), we find that $\chi_{m,n}^{\pm}$ satisfies the following recurrence relations,

$$\chi_{0,n}^{\pm} = \frac{1}{\mu^2 + \left(n + \frac{5}{2} + p_2\right)^2} \binom{n+p_{12}+4}{n}, \quad (3.35)$$

$$\chi_{m+1,n}^{\pm} = \frac{(m+n+p_2+3 \mp i\kappa)(m+n+p_{12}+5)}{\mu^2 + \left(m+n+\frac{7}{2}+p_2\right)^2} \chi_{m,n}^{\pm}, \quad (3.36)$$

which can be solved as

$$\chi_{m,n}^{\pm} = \frac{(5+n+p_{12})_m (3+n+p_2 \mp i\kappa)_m}{\left(\frac{5}{2}+n+p_2-i\mu\right)_{m+1} \left(\frac{5}{2}+n+p_2+i\mu\right)_{m+1}} \binom{n+p_{12}+4}{n} \quad (3.37)$$

where $(z)_n \equiv \Gamma[z+n]/\Gamma[z]$ is the Pochhammer symbol. Therefore, we obtain the particular solution from Eq. (3.37) and Eq. (3.34). While resolving the double summation in Eq. (3.34) is a non-trivial challenge, we manage to perform at least one of the summations, which results in

$$\begin{aligned} \mathcal{G}_{\pm\pm}^{p_1 p_2} &= \frac{H^2 e^{\mp \frac{\pi}{2} i p_{12}} \Gamma(p_{12} + 5)}{2^{p_{12}+5}} \sum_{n=0}^{\infty} u_1^{n+p_{12}+5} \left(1 - \frac{1}{u_2}\right)^n \binom{n+p_{12}+4}{n} \\ &\times \frac{1}{\mu^2 + \left(\frac{5}{2}+n+p_2\right)^2} {}_3F_2 \left[\begin{matrix} 1, 3+n+p_2 \mp i\kappa, 5+n+p_{12} \\ \frac{7}{2}+n+p_2-i\mu, \frac{7}{2}+n+p_2+i\mu \end{matrix} \middle| u_1 \right]. \end{aligned} \quad (3.38)$$

Finally, we note that the particular solution (3.38) automatically satisfies the second inhomogeneous differential equation with respect to u_2 (3.25). This is confirmed by substituting the ansatz (3.34) into Eq. (3.25). Then, in the same way as above, we obtain recurrence relations for $\chi_{m,n}$,

$$\chi_{0,n}^{\pm} = \frac{1}{\mu^2 + \left(n + \frac{5}{2} + p_2\right)^2} \binom{n+p_{12}+4}{n}, \quad (3.39)$$

$$\chi_{m+1,n}^{\pm} = \frac{(n+1)(n+3+p_2 \mp i\kappa)}{\mu^2 + (p_2+n+5/2)^2} \chi_{m,n+1}^{\pm}. \quad (3.40)$$

The first relation is exactly the same as Eq. (3.35) and one can check the second relation is automatically satisfied by our solution (3.37). Therefore, Eq. (3.38) gives a particular solution for both inhomogeneous differential equations (3.23) and (3.25).

Determining coefficients

We will specify boundary conditions for the seed integrals (3.1) to determine the coefficients \mathcal{C} in Eqs. (3.27) and (3.32). In Appendix A, we evaluated the seed integrals in the hierarchical collapsed limit ($u_1 \ll u_2 \ll 1$) by employing another method based on the Mellin–Barnes representation of the Whittaker function [128, 132]. The results are given by

$$\lim_{u_1 \ll u_2 \ll 1} \mathcal{I}_{\pm\mp}^{p_1 p_2} = \sum_{a,b=\pm} \tilde{\mathcal{C}}_{\pm\mp|ab} \tilde{\mathcal{U}}_{\pm|a}^{p_1}(u_1) \tilde{\mathcal{U}}_{\mp|b}^{p_2}(u_2), \quad (3.41)$$

$$\lim_{u_1 \ll u_2 \ll 1} \mathcal{I}_{\pm\pm}^{p_1 p_2} = \sum_{a,b=\pm} \tilde{\mathcal{C}}_{\pm\pm|ab} \tilde{\mathcal{U}}_{\pm|a}^{p_1}(u_1) \tilde{\mathcal{U}}_{\pm|b}^{p_2}(u_2), \quad (3.42)$$

where

$$\tilde{\mathcal{U}}_{a|b}^p(u) = iab 2^{iab\mu} \pi \operatorname{csch}(2\pi\mu) \left(\frac{u}{2}\right)^{5/2+p+iab\mu} \Gamma\left[\frac{5}{2} + p + iab\mu, \frac{1}{2} - ia\kappa + iab\mu\right], \quad (3.43)$$

and

$$\tilde{\mathcal{C}}_{\pm\mp|++} = \tilde{\mathcal{C}}_{\pm\mp|+-} = \tilde{\mathcal{C}}_{\pm\mp|-+} = \tilde{\mathcal{C}}_{\pm\mp|--} = \frac{e^{\pi\kappa}}{2\pi^2} H^2 [\cosh(2\pi\kappa) + \cosh(2\pi\mu)] e^{\mp i\pi\bar{p}_{12}/2}, \quad (3.44)$$

$$\tilde{\mathcal{C}}_{\pm\pm|++} = \tilde{\mathcal{C}}_{\pm\pm|+-} = \frac{\pm i e^{\pi(\kappa+\mu)} \cosh \pi(-\mu + \kappa) H^2}{\pi \Gamma\left[\frac{1}{2} - i\mu \mp i\kappa, \frac{1}{2} + i\mu \mp i\kappa\right]} e^{\mp i\pi p_{12}/2}, \quad (3.45)$$

$$\tilde{\mathcal{C}}_{\pm\pm|-+} = \tilde{\mathcal{C}}_{\pm\pm|--} = \frac{\pm i e^{\pi(\kappa-\mu)} \cosh \pi(\mu + \kappa) H^2}{\pi \Gamma\left[\frac{1}{2} - i\mu \mp i\kappa, \frac{1}{2} + i\mu \mp i\kappa\right]} e^{\mp i\pi p_{12}/2} \quad (3.46)$$

with $\bar{p}_{12} \equiv p_1 - p_2$. On the other hand, in the limit $u_1 \ll u_2 \ll 1$, $\mathcal{U}_{a|b}^p(u)$ defined in Eq. (3.28) reduced to $\tilde{\mathcal{U}}_{a|b}^p(u)$, and thus Eqs. (3.27) and (3.32) have to coincide with Eqs. (3.41) and (3.42). Therefore, the coefficient is determined as $\mathcal{C}_{\pm\mp|ab} = \tilde{\mathcal{C}}_{\pm\mp|ab}$ and $\mathcal{C}_{\pm\pm|ab} = \tilde{\mathcal{C}}_{\pm\pm|ab}$. In the derivation, we used the fact that, in the limit $u_1 \ll u_2 \ll 1$, the particular solution (3.38) is negligible compared to the second term in Eq. (3.32). This is because the particular solution behaves as $\sim u_1^{5+p_{12}} u_2^{5/2+p_2 \pm i\mu}$ in the collapsed limit, whereas scales for the dominant term is $\sim u_1^{5/2+p_1 \pm i\mu} u_2^{5/2+p_2 \pm i\mu}$.

Summary

In summary, the analytic expressions of the seed integrals (3.1) are obtained as follows:

$$\begin{aligned}
& \mathcal{I}_{\pm\mp}^{p_1 p_2} / H^2 \\
&= \frac{-e^{\mp i \frac{\pi}{2} \bar{p}_{12}} e^{\pi \kappa} [\cosh(2\pi \kappa) + \cosh(2\pi \mu)]}{2 \sinh^2(2\pi \mu)} \\
&\times \left\{ 2^{\pm i \mu} \left(\frac{u_1}{2} \right)^{\frac{5}{2} + p_1 \pm i \mu} {}_2\mathcal{F}_1 \left[\begin{matrix} \frac{5}{2} + p_1 \pm i \mu, \frac{1}{2} \mp i \kappa \pm i \mu \\ 1 \pm 2i \mu \end{matrix} \middle| u_1 \right] - (\mu \rightarrow -\mu) \right\} \\
&\times \left\{ 2^{\pm i \mu} \left(\frac{u_2}{2} \right)^{\frac{5}{2} + p_2 \pm i \mu} {}_2\mathcal{F}_1 \left[\begin{matrix} \frac{5}{2} + p_2 \pm i \mu, \frac{1}{2} \pm i \kappa \pm i \mu \\ 1 \pm 2i \mu \end{matrix} \middle| u_2 \right] - (\mu \rightarrow -\mu) \right\}, \tag{3.47}
\end{aligned}$$

$$\begin{aligned}
& \mathcal{I}_{\pm\pm}^{p_1 p_2} / H^2 \\
&= \frac{\mp i e^{\mp i \frac{\pi}{2} p_{12}} e^{\pi \kappa} \pi}{\Gamma \left[\frac{1}{2} \mp i \kappa - i \mu, \frac{1}{2} \mp i \kappa + i \mu \right] \sinh^2(2\pi \mu)} \\
&\times \left\{ \frac{e^{\pi \mu} \cosh[\pi(-\mu + \kappa)]}{2^{\mp i \mu}} \left(\frac{u_1}{2} \right)^{\frac{5}{2} + p_1 \pm i \mu} {}_2\mathcal{F}_1 \left[\begin{matrix} \frac{5}{2} + p_1 \pm i \mu, \frac{1}{2} \mp i \kappa \pm i \mu \\ 1 \pm 2i \mu \end{matrix} \middle| u_1 \right] - (\mu \rightarrow -\mu) \right\} \\
&\times \left\{ 2^{\pm i \mu} \left(\frac{u_2}{2} \right)^{\frac{5}{2} + p_2 \pm i \mu} {}_2\mathcal{F}_1 \left[\begin{matrix} \frac{5}{2} + p_2 \pm i \mu, \frac{1}{2} \mp i \kappa \pm i \mu \\ 1 \pm 2i \mu \end{matrix} \middle| u_2 \right] - (\mu \rightarrow -\mu) \right\} \\
&+ \frac{e^{\mp i \frac{\pi}{2} p_{12}} \Gamma(p_{12} + 5)}{2^{p_{12} + 5}} \sum_{n=0}^{\infty} u_1^{n + p_{12} + 5} \left(1 - \frac{1}{u_2} \right)^n \binom{n + p_{12} + 4}{n} \\
&\times \frac{1}{\mu^2 + \left(\frac{5}{2} + n + p_2 \right)} {}_2\mathcal{F}_2 \left[\begin{matrix} 1, 3 + n + p_2 \mp i \kappa, 5 + n + p_{12} \\ \frac{7}{2} + n + p_2 - i \mu, \frac{7}{2} + n + p_2 + i \mu \end{matrix} \middle| u_1 \right]. \tag{3.48}
\end{aligned}$$

where the definition of ${}_2\mathcal{F}_1$ is found in Eq. (3.29) and we remind $p_{12} \equiv p_1 + p_2$ and $\bar{p}_{12} \equiv p_1 - p_2$. These are the generalization from the results for constant mass [128, 132] to those with time-dependent mass. In fact, they reproduce the results for constant mass when $g(\phi) = m_0^2$, which formally corresponds to take $\kappa = 0$ (see Appendix B).

Before going to the three- and two-point correlation functions, let us comment on the momentum dependence of the seed integrals. These are the functions of u_1 and u_2 , and the same is true for constant mass. However, as already mentioned, they also depend on v defined in Eq. (2.9) through μ and κ (see Eq. (2.16)) because of the time-dependent σ -mass. Incorporating this effect into correlation functions is one of the main results of this work, and its impact on cosmological observables will be investigated in the next section. In the following, this additional momentum dependence of the seed integrals is explicitly denoted by $\mathcal{I}_{ab}^{p_1 p_2}(u_1, u_2, v(k_s))$.

3.3 Soft limit

The three-point correlation function (2.34) is obtained by taking the soft limit $k_4 \rightarrow 0$ ($u_2 \rightarrow 1$) of the seed integrals. For the two-point correlation function (2.35), we further take $k_2 \rightarrow 0$ ($u_1 \rightarrow 1$) corresponding to the double soft limit. These limits are non-trivial at first sight because of the cancellation of some apparent divergences [128, 132], so we look at it in detail in the following.

Single soft limit

In the single soft limit $k_4 \rightarrow 0$ ($u_2 \rightarrow 1$), the opposite sign seed becomes

$$\mathcal{I}_{\pm\mp}^{p_1 p_2}(u_1, 1, v(k_3)) = \tilde{\mathcal{C}}_{\pm\mp|++} \left(\mathcal{U}_{\pm|+}^{p_1}(u_1) + \mathcal{U}_{\pm|-}^{p_1}(u_1) \right) \left(U_{\mp|+}^{p_2} + U_{\mp|-}^{p_2} \right), \quad (3.49)$$

where $\tilde{\mathcal{C}}_{\pm\mp|++}$ is given in Eq. (3.44), and we defined

$$U_{a|b}^p \equiv \text{Fin.} \left\{ \mathcal{U}_{a|b}^p(1) \right\} = \frac{\text{iab}\pi}{2^{5/2+p}} \text{csch}(2\pi\mu) \Gamma \left[\begin{matrix} p + \frac{5}{2} + \text{iab}\mu, \frac{1}{2} + \text{iab}\mu - \text{ia}\kappa, -2 - p + \text{ia}\kappa \\ -\frac{3}{2} - p + \text{iab}\mu, \frac{1}{2} + \text{iab}\mu + \text{ia}\kappa \end{matrix} \right]. \quad (3.50)$$

The $\text{Fin.}\{\dots\}$ denotes the finite parts of $\mathcal{U}_{a|b}^p(1)$, and the divergence is canceled out in the combination $\mathcal{U}_{\mp|+}^{p_2}(1) + \mathcal{U}_{\mp|-}^{p_2}(1)$. In the same way, for the same sign seed, we have

$$\begin{aligned} \mathcal{I}_{\pm\pm}^{p_1 p_2}(u_1, 1, v(k_3)) \\ = \mathcal{G}_{\pm\pm}^{p_1 p_2}(u_1, 1, v(k_3)) + \left(\tilde{\mathcal{C}}_{\pm\pm|++} \mathcal{U}_{\pm|+}^{p_1}(u_1) + \tilde{\mathcal{C}}_{\pm\pm|+-} \mathcal{U}_{\pm|-}^{p_1}(u_1) \right) \left(U_{\pm|+}^{p_2} + U_{\pm|-}^{p_2} \right), \end{aligned} \quad (3.51)$$

in the limit $k_4 \rightarrow 0$ ($u_2 \rightarrow 1$), where $\tilde{\mathcal{C}}_{\pm\pm|++}$ and $\tilde{\mathcal{C}}_{\pm\pm|+-}$ are given in Eqs. (3.45) and (3.46). For the first term $\mathcal{G}_{\pm\pm}^{p_1 p_2}$, only $n = 0$ of the n -summation in Eq. (3.38) survives in the limit $u_2 \rightarrow 1$, and we obtain the expression without the infinite summation,

$$\mathcal{G}_{\pm\pm}^{p_1 p_2}(u_1, 1, v(k_3)) = \frac{H^2 e^{\mp \frac{\pi}{2} \text{i} p_{12}} \Gamma(p_{12} + 5) u_1^{p_{12}+5}}{2^{p_{12}+5} \left[\mu^2 + \left(p_2 + \frac{5}{2} \right)^2 \right]} {}_3F_2 \left[\begin{matrix} 1, 5 + p_{12}, 3 + p_2 \mp \text{i}\kappa \\ \frac{7}{2} + p_2 - \text{i}\mu, \frac{7}{2} + p_2 + \text{i}\mu \end{matrix} \middle| u_1 \right]. \quad (3.52)$$

In summary, after some simplification, we obtain

$$\begin{aligned}
& \mathcal{I}_{\pm\mp}^{p_1 p_2}(u_1, 1, v(k_3)) / H^2 \\
&= \left\{ \frac{e^{\mp i \frac{\pi}{2} \bar{p}_{12}} e^{\pi \kappa} \cosh[\pi(\mu - \kappa)]}{2^{\frac{5}{2} + p_2} \sinh(2\pi\mu)} \Gamma \left[\begin{matrix} -2 - p_2 \mp i\kappa, \frac{5}{2} + p_2 \pm i\mu \\ \frac{1}{2} + i\mu \mp i\kappa, \frac{1}{2} - i\mu \mp i\kappa, -\frac{3}{2} - p_2 \pm i\mu \end{matrix} \right] + (\mu \rightarrow -\mu) \right\} \\
&\quad \times \left\{ -2^{\pm i\mu} \left(\frac{u_1}{2} \right)^{\frac{5}{2} + p_1 \pm i\mu} \pi \operatorname{csch}(2\pi\mu) {}_2\mathcal{F}_1 \left[\begin{matrix} p_1 + \frac{5}{2} \pm i\mu, \frac{1}{2} \pm i\mu \mp i\kappa \\ 1 \pm 2i\mu \end{matrix} \middle| u_1 \right] + (\mu \rightarrow -\mu) \right\}, \tag{3.53}
\end{aligned}$$

$$\begin{aligned}
& \mathcal{I}_{\pm\pm}^{p_1 p_2}(u_1, 1, v(k_3)) / H^2 \\
&= \frac{e^{\mp i \frac{\pi}{2} p_{12}} \Gamma(5 + p_{12})}{2^{5 + p_{12}} \left[\mu^2 + \left(p_2 + \frac{5}{2} \right)^2 \right]} u_1^{5 + p_{12}} {}_3F_2 \left[\begin{matrix} 1, 3 + p_2 \mp i\kappa, 5 + p_{12} \\ \frac{7}{2} + p_2 - i\mu, \frac{7}{2} + p_2 + i\mu \end{matrix} \middle| u_1 \right] \\
&\quad \mp i \left\{ \frac{e^{\mp i \frac{\pi}{2} p_{12}} e^{\pi \kappa} \cosh[\pi(\mu + \kappa)]}{2^{\frac{5}{2} + p_2} \sinh(2\pi\mu)} \Gamma \left[\begin{matrix} -2 - p_2 \pm i\kappa, \frac{5}{2} + p_2 \pm i\mu \\ -\frac{3}{2} - p_2 \pm i\mu \end{matrix} \right] + (\mu \rightarrow -\mu) \right\} \\
&\quad \times \left\{ \left(\frac{u_1}{2} \right)^{\frac{5}{2} + p_1 \pm i\mu} \frac{e^{\pi \mu} \cosh[\pi(\mu - \kappa)]}{2^{\mp i\mu} \sinh(2\pi\mu)} {}_2\mathcal{F}_1 \left[\begin{matrix} p_1 + \frac{5}{2} \pm i\mu, \frac{1}{2} \pm i\mu \mp i\kappa \\ 1 \pm 2i\mu \end{matrix} \middle| u_1 \right] + (\mu \rightarrow -\mu) \right\}. \tag{3.54}
\end{aligned}$$

in the single soft limit $k_4 \rightarrow 0$. Here $\bar{p}_{12} \equiv p_1 - p_2$ and $p_{12} \equiv p_1 + p_2$. These reproduces the results for constant mass when $g(\phi) = m_0^2$ or $\kappa = 0$ (see Appendix B).

Double soft limit

To consider the double soft limit, we take a limit $k_2 \rightarrow 0$ ($u_1 \rightarrow 1$) of the expressions in single soft limit Eqs. (3.49) and (3.51). For the opposite sign seed, we have

$$\mathcal{I}_{\pm\mp}^{p_1 p_2}(1, 1, v(k_3)) = \tilde{\mathcal{C}}_{\pm\mp|++} \left(U_{\pm|+}^{p_1} + U_{\pm|-}^{p_1} \right) \left(U_{\mp|+}^{p_2} + U_{\mp|-}^{p_2} \right). \tag{3.55}$$

In the same way as the single soft limit, divergences are canceled in a combination, $\mathcal{U}_{\pm|+}^{p_1}(1) + \mathcal{U}_{\pm|-}^{p_1}(1)$. For the same sign seed, we have

$$\begin{aligned}
& \mathcal{I}_{\pm\pm}^{p_1 p_2}(1, 1, v(k_3)) \\
&= \text{Fin.} \{ \mathcal{G}_{\pm\pm}^{p_1 p_2}(1, 1, v(k_3)) \} + \left(\tilde{\mathcal{C}}_{\pm\pm|++} U_{\pm|+}^{p_1} + \tilde{\mathcal{C}}_{\pm\pm|+-} U_{\pm|-}^{p_1} \right) \left(U_{\pm|+}^{p_2} + U_{\pm|-}^{p_2} \right), \tag{3.56}
\end{aligned}$$

where

$$\text{Fin.} \{ \mathcal{G}_{\pm\pm}^{p_1 p_2}(1, 1, v(k_3)) \} = \frac{H^2 e^{\mp i \frac{\pi}{2} p_{12}} \Gamma(p_{12} + 5)}{2^{p_{12} + 5}} {}_3\mathcal{F}_2 \left[\begin{matrix} \frac{5}{2} + p_2 - i\mu, \frac{5}{2} + p_2 + i\mu, -2 - p_1 \pm i\kappa \\ 3 + p_2 \pm i\kappa, 1 - p_1 + p_2 \end{matrix} \middle| 1 \right]. \tag{3.57}$$

Here we used

$$\text{Fin.} \left\{ \lim_{u \rightarrow 1} {}_3F_2 \left[\begin{matrix} a, b, c \\ d, e \end{matrix} \middle| u \right] \right\} = \Gamma \left[\begin{matrix} d, e, s \\ c, a + s, b + s \end{matrix} \right] {}_3F_2 \left[\begin{matrix} d - c, e - c, s \\ a + s, b + s \end{matrix} \middle| 1 \right], \quad (3.58)$$

where $s \equiv d + e - a - b - c$. In this case, cancellation of the divergence is not within the combination of $\tilde{\mathcal{C}}_{\pm\pm|++} \mathcal{U}_{\pm|+}^{p_1}(1) + \tilde{\mathcal{C}}_{\pm\pm|+-} \mathcal{U}_{\pm|-}^{p_1}(1)$, but with the one from $\mathcal{G}_{\pm\pm}^{p_1 p_2}(1, 1, v(k_3))$.

In summary, we obtain the double soft limit ($k_4, k_2 \rightarrow 0$) of the seed integrals as

$$\begin{aligned} & \mathcal{I}_{\pm\mp}^{p_1 p_2}(1, 1, v(k_3)) / H^2 \\ &= \frac{e^{\mp i \frac{\pi}{2} \bar{p}_{12}} e^{\pi \kappa}}{2^{5+p_{12}}} \Gamma \left[\begin{matrix} \frac{5}{2} + p_1 - i\mu, \frac{5}{2} + p_1 + i\mu, \frac{5}{2} + p_2 - i\mu, \frac{5}{2} + p_2 + i\mu \\ 3 + p_1 \mp i\kappa, 3 + p_2 \pm i\kappa \end{matrix} \right], \end{aligned} \quad (3.59)$$

$$\begin{aligned} & \mathcal{I}_{\pm\pm}^{p_1 p_2}(1, 1, v(k_3)) / H^2 \\ &= \Gamma \left[\begin{matrix} \frac{5}{2} + p_1 - i\mu, \frac{5}{2} + p_1 + i\mu, \frac{5}{2} + p_2 - i\mu, \frac{5}{2} + p_2 + i\mu, \frac{1}{2} + i\mu \mp i\kappa, \frac{1}{2} - i\mu \mp i\kappa \\ 3 + p_1 \mp i\kappa, 3 + p_2 \pm i\kappa \end{matrix} \right] \\ & \quad \times \frac{\pm i e^{\mp i \frac{\pi}{2} p_{12}} (e^{-2\pi\mu} + e^{2\pi\kappa})}{2^{6+p_{12}} \pi} \\ & \quad - \frac{e^{\mp i \frac{\pi}{2} p_{12}}}{2^{5+p_{12}}} \Gamma \left[\begin{matrix} \frac{5}{2} + p_1 \pm i\mu, \frac{5}{2} + p_2 \pm i\mu \\ \frac{1}{2} \pm i\mu \pm i\kappa \end{matrix} \right] {}_3\mathcal{F}_2 \left[\begin{matrix} \frac{1}{2} \pm i\mu \pm i\kappa, 5 + p_{12}, 1 \\ \frac{7}{2} + p_1 \pm i\mu, \frac{7}{2} + p_2 \pm i\mu \end{matrix} \middle| 1 \right]. \end{aligned} \quad (3.60)$$

As we expected, they reproduce the results for constant mass when $g(\phi) = m_0^2$ or $\kappa = 0$ (see Appendix B).

4 Impact on Primordial non-Gaussianity

With the analytical expressions for the seed integrals (3.47) and (3.48), as well as their soft limits (3.53), (3.54), (3.59), and (3.60), we are now ready to compute the inflationary correlators by using Eqs. (2.32), (2.34), and (2.35). This section will discuss phenomenology observed in the scale-dependent power spectrum and bispectrum.

To provide a clear and concrete framework for the subsequent discussion, we assume a specific interaction

$$g(\phi) = m_0^2 \left(1 + \alpha \frac{\phi}{M_{\text{Pl}}} \right), \quad (4.1)$$

unless explicitly stated otherwise. The first term represents a time-independent bare mass of σ , and the second term introduces an inflaton (or time) dependence. In the expression, α is a time-independent coupling constant, and the limit $\alpha \rightarrow 0$ realizes a constant mass scenario. We also note that Eq. (4.1) can be considered as the leading expansion of $e^{\alpha\phi/M_{\text{Pl}}}$,

whose impact on the bispectrum was explored numerically in Ref. [86]. In this context, the parameters μ and κ in Eq. (2.16) are

$$\mu^2(v) = \frac{m_0^2}{H^2} \left(1 - \sqrt{2\epsilon}\alpha \log v - \sqrt{2\epsilon}\alpha \right) - \frac{9}{4}, \quad \kappa = -\frac{\sqrt{2\epsilon}\alpha m_0^2}{2H^2}. \quad (4.2)$$

Furthermore, to avoid a tachyonic mass for σ , we focus on the following parameter region,

$$|\log v| \lesssim \frac{1}{\sqrt{2\epsilon}|\alpha|}. \quad (4.3)$$

4.1 Power spectrum

The power spectrum P_ζ is defined by

$$\langle \zeta_{\mathbf{k}_1} \zeta_{\mathbf{k}_3} \rangle' \equiv \frac{2\pi^2}{k_1^3} P_\zeta, \quad (4.4)$$

where the prime denotes the omission of the momentum conservation factor. The curvature perturbation ζ is related to the inflaton fluctuation $\delta\phi$ by⁵

$$\zeta = -\frac{H}{\dot{\phi}_0} \delta\phi = \frac{1}{\sqrt{2\epsilon}M_{\text{Pl}}} \delta\phi. \quad (4.5)$$

As is well established, the standard expression for the power spectrum at leading order is given by

$$P_\zeta^{(0)} = \frac{H^4}{4\pi^2 \dot{\phi}_0^2} = \frac{H^2}{8\pi^2 \epsilon M_{\text{Pl}}^2}, \quad (4.6)$$

and scale dependence appears as slow-roll corrections. In our scenario, Eq. (2.35) combined with Eq. (4.5) introduces a correction to the power spectrum,

$$P_\zeta^{(1)} = \frac{1}{16\pi^2} \cdot \frac{c_2^2}{H^2 M_{\text{Pl}}^2} \sum_{a,b=\pm} \mathcal{I}_{ab}^{-2,-2}(1, 1, v(k_1)), \quad (4.7)$$

where $\mathcal{I}_{ab}^{p_1,p_2}$ with double soft limit are shown in Eqs. (3.59) and (3.60). The correction from a constant mass scalar field was initially computed analytically in Ref. [17] through direct integration. The same outcome was subsequently derived by solving the bootstrap equations in Ref. [128, 132]. As a consistency check, our result (4.7) reproduces the result in the constant mass limit, i.e., $\alpha = 0$. Note that, in contrast to the constant mass case where

⁵In our analysis, we consider a simple scenario in which the curvature perturbation solely arises from inflaton fluctuation, without involving more complicated situations such as curvaton or modulated reheating scenarios.

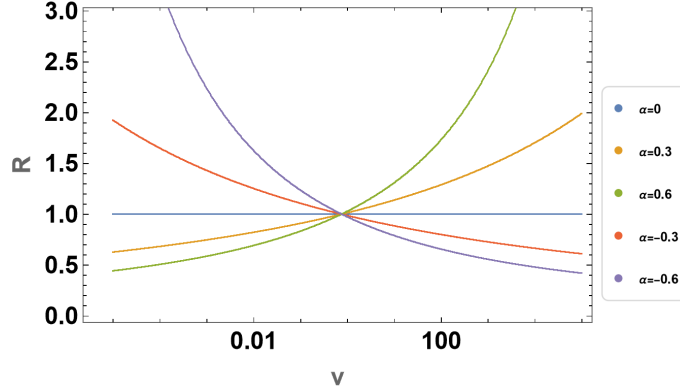


Figure 2 $v(k_1)(=k_1/k_0)$ -dependence of R . We fix $m_0 = 2H$ and $\epsilon = 0.05/16$, and change the parameter α from -0.6 to 0.6 .

$P_\zeta^{(1)}$ is scale-invariant, Eq. (4.7) depends on the specific momentum ratio $v(k_1) = k_1/k_0$, due to the time-dependent nature of the σ -mass.

To see these effects, we introduce a ratio,

$$R \equiv \frac{P_\zeta^{(1)}}{P_\zeta^{(1)}(\alpha = 0)}, \quad (4.8)$$

with the denominator representing the correction to the power spectrum in case of a constant mass. In Fig. 2, we plot the variation of R as a function of $v(k_1)$. Our choice of parameter includes a fixed $m_0 = 2H$ and $\epsilon = 0.05/16$, with α ranging from -0.6 to 0.6 . Depending on the values of v and α , the correction to the power spectrum can either be increased or decreased. Furthermore, we can analytically estimate the leading v -dependence of the power spectrum $P_\zeta^{(1)}$ as

$$\frac{\partial P_\zeta^{(1)}}{\partial v} = f_P(m_0) \frac{\sqrt{\epsilon} \alpha}{v} + \mathcal{O}(\epsilon), \quad (4.9)$$

where $f_P(m_0)$ is a function of m_0 . This v dependence coincides with the behavior derived in general single field inflation scenarios (see e.g., [151]). Note that, although the v -dependence is identical, the leading order of slow-roll parameter dependence is different from the general single field case where the leading order is $\mathcal{O}(\epsilon, \eta)$. We also note that the v -dependence in Eq. (4.9) is universal as slow-roll correction, while the effect of σ -field on the inflation background is highly model-dependent. For instance, the power spectrum can often be expanded as $P_\zeta = P_{\zeta*} + \epsilon(t_{\text{exit}} - t_*) + \mathcal{O}(\epsilon^2) \sim P_{\zeta*} + \epsilon \log(k/k_*)$ where ϵ represents the leading slow-roll order of the theory, e.g., $\epsilon = \mathcal{O}(\sqrt{\epsilon})$ in our case.

4.2 Bispectrum

The bispectrum is characterized by the so-called shape function S defined by

$$\langle \zeta_{\mathbf{k}_1} \zeta_{\mathbf{k}_2} \zeta_{\mathbf{k}_3} \rangle' \equiv (2\pi)^4 \frac{P_\zeta^2}{(k_1 k_2 k_3)^2} S. \quad (4.10)$$

Combining Eq. (2.34) with Eq. (4.5), we derive the shape function

$$S = \frac{1}{(2\pi)^4} \cdot \frac{1}{P_\zeta^2} \cdot (2\epsilon M_{\text{Pl}}^2)^{-\frac{3}{2}} \cdot (-2c_2 c_3) \cdot \frac{H}{8} \sum_{a,b=\pm} \left[\frac{k_1 k_2}{k_3^2} \mathcal{I}_{ab}^{0,-2} \left(\frac{2k_3}{k_{123}}, 1, v(k_3) \right) + 2\text{per.} \right], \quad (4.11)$$

where the single soft limit of $\mathcal{I}_{ab}^{p_1 p_2}$ is described in Eqs. (3.53) and (3.54). In the subsequent subsections, we explore the behavior of the shape function in detail.

4.2.1 Cosmological collider signal at squeezed configuration

Let us consider the configuration $k_1 = k_2$, and define $x \equiv k_3/k_{1,2}$ and $v \equiv k_1/k_0$. Consequently, we can express Eq. (4.11) as

$$S = \frac{1}{(2\pi)^4} \cdot \frac{1}{P_\zeta^2} \cdot (2\epsilon M_{\text{Pl}}^2)^{-\frac{3}{2}} \cdot (-2c_2 c_3) \cdot \frac{H}{8} \times \sum_{a,b=\pm} \left[\frac{1}{x^2} \mathcal{I}_{ab}^{0,-2} \left(\frac{2x}{2+x}, 1, vx \right) + 2x \mathcal{I}_{ab}^{0,-2} \left(\frac{2}{2+x}, 1, v \right) \right]. \quad (4.12)$$

In this expression, the squeezed limit $k_3 \ll k_{1,2}$ corresponds to $x \ll 1$, while the equilateral one $k_1 \simeq k_2 \simeq k_3$ to $x \simeq 1$.

The squeezed limit of the bispectrum is of particular interest in cosmological collider physics, as specific oscillatory patterns can sharply appear in this limit. In Fig. 3, we present $S/c_2 c_3 \sqrt{x}$ as a function of x^{-1} , with varying values of α . Our parameter choices are $v = 1$, $m_0 = 2H$ ($2.5H$) for $\alpha > 0$ (< 0), $\epsilon = 0.05/16$, and $M_{\text{Pl}}/H = 10^5$.⁶ It is readily apparent that both the amplitude and the oscillation frequency exhibit strong dependence on k_1/k_3 . For $\alpha > 0$, the amplitude experiences damping and the frequency diminish in the squeezed configuration ($x \ll 1$). The opposite behavior is observed for $\alpha < 0$. This feature is more prominent for an increased value of $|\alpha|$, and the deviation from a constant mass signal is sufficiently significant to observe. Note that these results are consistent with previous works, including calculations within super-horizon approximation [70] and numerical simulation [86].

The physical interpretation of this signal is clear. In the squeezed limit $x \ll 1$, we are essentially observing the correlation between a long wavelength mode k_3 and short ones $k_{1,2}$.

⁶We use these values of ϵ and M_{Pl}/H in all figures below.

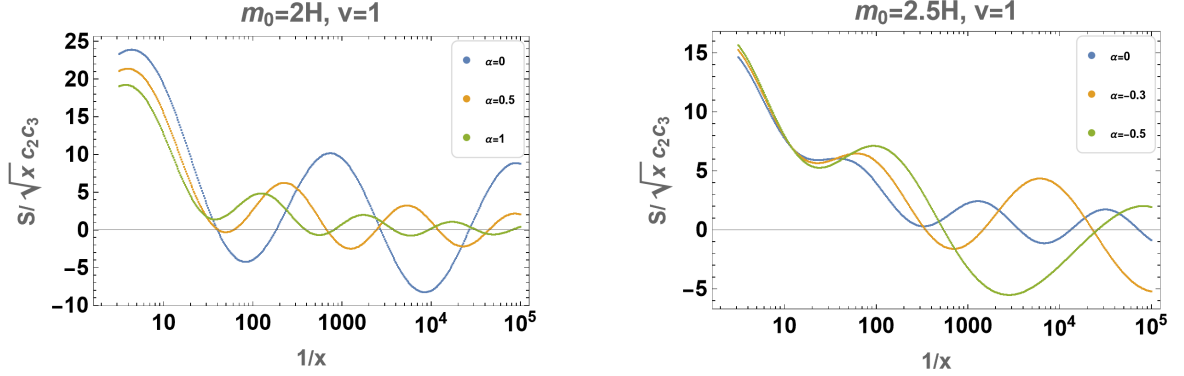


Figure 3 $S/c_2c_3\sqrt{x}$ as a function of x^{-1} with several choices of α . *Left* : Case with $\alpha \geq 0$, that is changed as 0 (blue), 0.5 (orange), and 1 (green). *Right* : Case with $\alpha \leq 0$, that is changed as 0 (blue), -0.3 (orange), and -0.5 (green).

The long mode exits the horizon earlier than the short ones and evolves on the super-horizon scale $|k_3\tau| \ll 1$, schematically represented by

$$v_{k_3}(\tau) \sim (-\tau)^{\frac{3}{2}} \left[(-\tau)^{i\mu} + e^{-\pi\mu} (-\tau)^{-i\mu} \right], \quad (4.13)$$

where we showed only τ -dependence of the mode function, disregarding the relative phase of the positive and negative frequency modes. The relative amplitude $e^{-\pi\mu}$ of the positive and negative frequency modes is nothing but (the square root of) the Boltzmann factor responsible for on-shell particle creation relevant to the CC signal. In the present case, μ exhibits scale dependence due to the horizon crossing time difference. For $\alpha > 0$ (< 0), the mass of σ becomes heavier (lighter) than the constant mass scenario due to its time-dependent nature. Consequently, the mode function is more (less) suppressed by the Boltzmann factor $e^{-\pi\mu}$ compared to the constant mass case, leading to a smaller (larger) amplitude and a shorter (longer) wavelength in the oscillatory signal of the bispectrum. Furthermore, the oscillation frequency is scale-dependent accordingly.

4.2.2 Distinction of couplings with inflaton

Recall that the time-dependent mass appears because the non-derivative couplings break the shift symmetry; it is not easy to obtain similar effects from derivative couplings. Therefore, when we observe the specific behavior in the CC signal, such as the damping/enhancement of amplitude and the shrinking/spreading of wavelength in the squeezed limit, it is attributed to these non-derivative (direct) interactions. Moreover, detailed observations of the time-dependent Boltzmann factor associated with non-derivative couplings between the inflaton and the σ -field allow us to distinguish the form of the interactions. This is obtained from distinctive characteristics in the tail of the “scaling” behavior in the CC signal. We will delve deeper into this aspect in the following discussion.

In the shape function (4.12) with Eqs. (3.53) and (3.54), one can extract the Boltzmann factor for $\mu \gtrsim 1$ with

$$|\Gamma(a + ib)| \sim e^{-\pi|b|/2}, \quad |b| \gtrsim 1, \quad a, b \in \mathbb{R}, \quad (4.14)$$

This reveals that the shape function behaves as

$$S/\sqrt{x} \sim e^{-\pi\mu(x)} x^{\pm i\mu} + \text{c.c.}, \quad (4.15)$$

in the squeezed limit, $x \ll 1$ ⁷. Regarding the Boltzmann factor $e^{-\pi\mu(x)}$, it is crucial to emphasize that μ exhibits x -dependence due to the time-dependent mass arising from the coupling to the inflaton, unlike the constant mass situation⁸. Consequently, the amplitude of the CC signal exhibits a scaling behavior in addition to the well-known oscillation, as observed in the previous subsection (see Fig. 3). In case of the linear coupling (4.1), we can estimate the scaling

$$e^{-\pi\mu(x)} \sim e^{-\pi m_0/H} \cdot \left(\frac{v}{x}\right)^{-\pi \frac{m_0}{H} \sqrt{\frac{\epsilon}{2}} \alpha}, \quad (4.16)$$

as a function of x . The left figure of Fig. 4 illustrates the scaling tail of the oscillatory part (orange line) estimated in Eq. (4.16) on the top of the full shape including the background part (4.12). Eq. (4.16) essentially characterizes the scaling behavior in the squeezed limit ($x \ll 1$).

Remarkably, the scaling behavior exhibits dependence on the coupling between the inflaton and the massive field. For example, in the case of a quadratic coupling,

$$g(\phi) = m_0^2 \left(1 + \beta \frac{\phi^2}{M_{\text{Pl}}^2}\right), \quad (4.17)$$

we obtain

$$e^{-\pi\mu(x)} \sim e^{-\pi m_0/H} \cdot e^{-\pi \frac{m_0}{H} \cdot \beta \epsilon (\log vx) (\log vx + 2)} \quad (4.18)$$

instead of Eq. (4.16). This new formulation represents the amplitude of the corresponding CC signal, as demonstrated in the right panel of Fig. 4, and the scaling behavior (x -dependence) differs significantly from the linear case. Therefore, in principle, we can distinguish the coupling $g(\phi)$ through careful observations and analysis of these scaling behaviors.

It is straightforward to obtain a similar formula for more generic couplings. For example, for a coupling,

$$g(\phi) = m_0^2 \left(1 + \alpha_{(n)} \frac{\phi^n}{M_{\text{Pl}}^n}\right), \quad (4.19)$$

⁷In Eq. (4.12), the dominance of the first term over the second one holds true for $x \ll 1$.

⁸One may expect the existence of so-called chemical potential [69, 75] from the expression of the mode function (2.17). However, the approximation (2.11) is valid only in the parameter region where the effect of chemical potential is negligible, $e^{\pi(\kappa - \mu)} \sim e^{-\pi\mu}$, which is our focus throughout this paper.

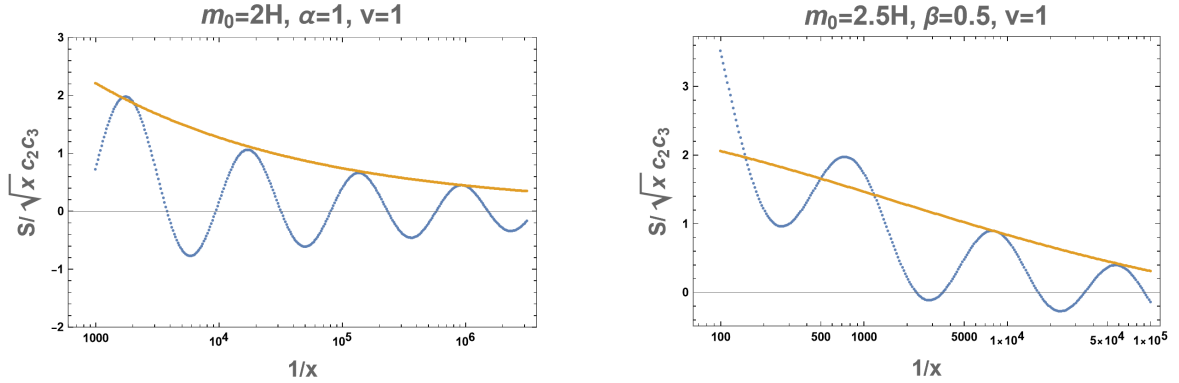


Figure 4 Fitting of the full shape (4.12) (blue line) with scaling function $e^{-\pi\mu(x)}$ (orange line). *Left* : Linear case (4.1) with Eq. (4.16). *Right* : Quadratic case (4.17) with (4.18). Parameters are chosen as described in the figure.

with n being positive integers, we have the following scaling function,

$$e^{-\pi\mu(x)} \sim e^{-\pi m_0/H} \cdot e^{-\pi \frac{m_0}{H} \cdot \frac{\alpha(n)}{2} (-\sqrt{2\epsilon})^n (\log vx)^{n-1} (\log vx + n)}, \quad (4.20)$$

which predicts a different scaling depending on n .

4.2.3 Equilateral configuration

While the CC signal in the squeezed configuration is quite essential to extract information about σ -field, the bispectrum (4.12) exhibits a peak (dominant contribution) at the equilateral limit $x \simeq 1$. Hence, it is equally valuable to investigate the behavior around the equilateral configuration. In our scenario, the magnitude of the shape function or the non-Gaussianity parameter f_{NL} in the equilateral limit is estimated by using

$$f_{\text{NL}}^{\text{equi}} \sim c_2 c_3 \times \mathcal{O}(10), \quad (4.21)$$

for $\alpha \sim \mathcal{O}(1)$ and $m_0 \sim \mathcal{O}(H)$.

In Fig. 5, we present plots of S for $x \gtrsim 0.1$ (equilateral configuration) varying the interaction strength α (left figure) and the additional scale dependence v (right figure). We find that the values of α and v change the scaling behavior of the bispectrum towards the equilateral configuration. Furthermore, the leading v -dependence of the shape function S at $x = 1$ is obtained in the same way as the power spectrum. Specifically, $\partial S / \partial v = f_S(m_0) \sqrt{\epsilon} \alpha / v + \mathcal{O}(\epsilon)$ where $f_S(m_0)$ is a function of m_0 . Unfortunately, for reasons discussed in the subsection of the power spectrum, it is difficult to extract information about the theory from the scale dependence at the exact equilateral configuration.

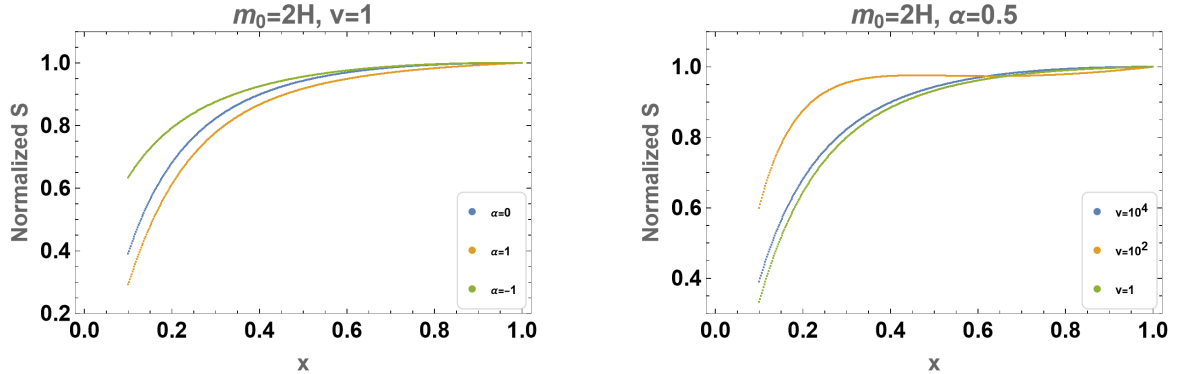


Figure 5 The shape function S as the function of x . Here S is normalized to have value 1 at the equilateral limit $x = 1$. *Left:* α -dependence with $m_0 = 2H$ and $v = 1$ fixed. *Right:* v -dependence with $m_0 = 2H$ and $\alpha = 0.5$ fixed.

5 Summary

Our paper provided analytical formulae for the inflationary correlators, specifically two-, three-, and four-point correlation functions, in the presence of a massive scalar field with time-dependent mass. The results are summarized in Eqs. (3.47) and (3.48) for four-point correlators, Eqs. (3.53) and (3.54) for three-point, and Eqs. (3.59) and (3.60) for two-point. The time dependence of mass naturally arises from couplings to the inflaton, and its effects can be significant when the couplings do not respect the shift symmetry of the inflaton, i.e., in the case of non-derivative couplings. The mode function of the massive field (2.17) is analytically given by the Whittaker function under the linear order expansion around the time of horizon crossing for the time-dependence inflaton background, which characterizes the scale dependence of the signal. The analytical formulae for the correlators obtained from the bootstrap method include both the signal (oscillatory) parts and the background (non-oscillatory) parts of the bispectrum as graphically shown in Fig. 3 and 5. The non-oscillatory part of the signal is also crucial for achieving precision in the cosmological collider (CC) program.

As an application, the phenomenological impact of the time dependence on the primordial curvature power spectrum and bispectrum were investigated. Our analysis revealed that the CC signal exhibits the damping/enhancement of amplitude due to the time-dependent (or scale-dependent) Boltzmann factor. The change in amplitude in the CC signal can be readily observed and provide evidence for the time-dependent mass of the massive field. Although this behavior has been qualitatively confirmed in previous numerical studies such as Ref. [86], we quantitatively parameterized this scaling of the amplitude in a simple form (4.20) based on our analytical formulae. By probing the scaling behavior in the tail of the signal, we are able to distinguish couplings between the inflaton and the massive field, which provides a pathway to explore the unknown inflaton sector through the CC signal.

It should be noted that we made an approximation by linearizing the time dependence of the inflaton and omitting the higher-order time dependence. This is merely the approximation made in our study. While extensions beyond linear order present technical challenges in obtaining analytical representations of non-Gaussianity, there are interesting scenarios beyond the scope of our setup, such as CC signals from tachyonic phase transitions [48]. We plan to explore these topics in future work.

Acknowledgments

We thank Lucas Pinol, Yi Wang and Zhong-Zhi Xianyu for valuable discussions and their hospitalities when F.S. stayed at their groups, Dong-Gang Wang and Sébastien Renaux-Petel for valuable discussions in Gravity 2023, YITP and COSMO 2023, IFT, and Yuhang Zhu for valuable discussions. S.A. is supported by IBS under the project code, IBS-R018-D1. T.N. is supported in part by JSPS KAKENHI Grant No. 20H01902 and No. 22H01220, and MEXT KAKENHI Grant No. 21H05184 and No. 23H04007. F.S. is supported by financial aid from the Center for the Theoretical Physics of the Universe, Institute for Basic Science, financial aid from the Advanced Research Center for Quantum Physics and Nanoscience, Tokyo Institute of Technology, and JSPS Grant-in-Aid for Scientific Research No. 23KJ0938. M.Y. is supported by IBS under the project code IBS-R018-D3 and JSPS Grant-in-Aid for Scientific Research No. JP21H01080.

A Seed integral with the Mellin–Barnes representation

In this appendix, we present a direct integration method for the seed integral (2.33), based on the technique utilized in Ref. [128, 132] which makes use of the Mellin–Barnes representation of Whittaker function,

$$W_{\kappa,\nu}(z) = e^{z/2} \int_{-i\infty}^{+i\infty} \frac{ds}{2\pi i} \Gamma \left[\begin{matrix} s - \nu, s + \nu \\ s - \kappa + \frac{1}{2} \end{matrix} \right] z^{-s+1/2}, \quad (\text{A.1})$$

$$W_{\kappa,\nu}(z) = e^{-z/2} \int_{-i\infty}^{+i\infty} \frac{ds}{2\pi i} \Gamma \left[\begin{matrix} s - \nu, s + \nu, -s - \kappa + \frac{1}{2} \\ \frac{1}{2} - \kappa - \nu, \frac{1}{2} - \kappa + \nu \end{matrix} \right] z^{-s+1/2}. \quad (\text{A.2})$$

As a reminder, the notation used in the paper is as follows:

$${}_p\mathcal{F}_q \left[\begin{matrix} a_1, \dots, a_p \\ b_1, \dots, b_q \end{matrix} \middle| z \right] \equiv \Gamma \left[\begin{matrix} a_1, \dots, a_p \\ b_1, \dots, b_q \end{matrix} \right] {}_pF_q \left[\begin{matrix} a_1, \dots, a_p \\ b_1, \dots, b_q \end{matrix} \middle| z \right], \quad (\text{A.3})$$

where ${}_pF_q$ represents the (generalized) hypergeometric function, and the products of gamma functions are abbreviated as

$$\Gamma[z_1, \dots, z_m] \equiv \Gamma(z_1) \cdots \Gamma(z_m), \quad (\text{A.4})$$

$$\Gamma \left[\begin{matrix} z_1, \dots, z_m \\ w_1, \dots, w_n \end{matrix} \right] \equiv \frac{\Gamma(z_1) \cdots \Gamma(z_m)}{\Gamma(w_1) \cdots \Gamma(w_n)}. \quad (\text{A.5})$$

Opposite sign seed $\mathcal{I}_{\pm\mp}^{p_1 p_2}$

To compute the opposite sign seed integral $\mathcal{I}_{\pm\mp}^{p_1 p_2}$, we first express the propagators $D_{\pm\mp}$ using Eq. (A.2):

$$\begin{aligned} D_{\pm\mp}(k; \tau_1, \tau_2) &= \frac{e^{\pi\kappa}}{2k} H^2(\tau_1 \tau_2) W_{\pm i\kappa, \mp i\mu}(\mp 2ik\tau_1) W_{\mp i\kappa, \pm i\mu}(\pm 2ik\tau_2) \\ &= \frac{e^{\pi\kappa}}{2\pi^2} H^2 e^{\pm i\kappa(\tau_1 - \tau_2)} [\cosh(2\pi\kappa) + \cosh(2\pi\mu)] \\ &\quad \times \int_{-i\infty}^{+i\infty} \frac{ds_1}{2\pi i} \frac{ds_2}{2\pi i} e^{\mp i\pi(s_1 - s_2)/2} (2k)^{-s_{12}} (-\tau_1)^{-s_1+3/2} (-\tau_2)^{-s_2+3/2} \\ &\quad \times \Gamma\left[-s_1 + \frac{1}{2} \mp i\kappa, -s_2 + \frac{1}{2} \pm i\kappa, s_1 - i\mu, s_1 + i\mu, s_2 - i\mu, s_2 + i\mu\right], \quad (\text{A.6}) \end{aligned}$$

where $s_{12} = s_1 + s_2$. Substituting this expression into $\mathcal{I}_{\pm\mp}^{p_1 p_2}$ enables us to carry out the $\tau_{1,2}$ -integral, resulting in

$$\begin{aligned} \mathcal{I}_{\pm\mp}^{p_1 p_2} &= \frac{e^{\pi\kappa(k_s)}}{2\pi^2} H^2 [\cosh(2\pi\kappa(k_s)) + \cosh(2\pi\mu)] \left(\frac{u_1}{2}\right)^{5/2+p_1} \left(\frac{u_2}{2}\right)^{5/2+p_2} e^{\mp i\pi(p_1 - p_2)/2} \\ &\quad \times \int_{-i\infty}^{i\infty} \frac{ds_1}{2\pi i} \frac{ds_2}{2\pi i} u_1^{-s_1} u_2^{-s_2} \Gamma\left[p_1 + \frac{5}{2} - s_1, p_2 + \frac{5}{2} - s_2\right] \\ &\quad \times \Gamma\left[-s_1 + \frac{1}{2} \mp i\kappa(k_s), -s_2 + \frac{1}{2} \pm i\kappa(k_s), s_1 - i\mu, s_1 + i\mu, s_2 - i\mu, s_2 + i\mu\right], \quad (\text{A.7}) \end{aligned}$$

where

$$u_1 \equiv \frac{2r_1}{1+r_1}, \quad u_2 \equiv \frac{2r_2}{1+r_2}, \quad (\text{A.8})$$

and we explicitly denote k_s dependence in $\kappa(k_s)$ (see Eq. (2.16) with Eq. (2.9)). The integration over s_i can be computed using the residue theorem. We close the contours from the left with a large semicircle and pick up the poles $s_i = -n_i \pm i\mu$ with n_i to be non-negative integers. This process allows us to express the seed integral as

$$\begin{aligned} \mathcal{I}_{\pm\mp}^{p_1 p_2} &= \frac{e^{\pi\kappa(k_s)}}{2\pi^2} H^2 [\cosh(2\pi\kappa(k_s)) + \cosh(2\pi\mu)] \left(\frac{u_1}{2}\right)^{5/2+p_1} \left(\frac{u_2}{2}\right)^{5/2+p_2} e^{\mp i\pi(p_1 - p_2)/2} \\ &\quad \times \sum_{n_1=0}^{\infty} \left\{ \frac{(-1)^{n_1}}{n_1!} u_1^{n_1+i\mu} \Gamma\left[n_1 + p_1 + \frac{5}{2} + i\mu, n_1 + i\mu + \frac{1}{2} \mp i\kappa(k_s), -n_1 - 2i\mu\right] + (\mu \rightarrow -\mu) \right\} \\ &\quad \times \sum_{n_2=0}^{\infty} \left\{ \frac{(-1)^{n_2}}{n_2!} u_2^{n_2+i\mu} \Gamma\left[n_2 + p_2 + \frac{5}{2} + i\mu, n_2 + i\mu + \frac{1}{2} \pm i\kappa(k_s), -n_2 - 2i\mu\right] + (\mu \rightarrow -\mu) \right\}, \quad (\text{A.9}) \end{aligned}$$

and the summations can be performed explicitly, leading to

$$\begin{aligned} \mathcal{I}_{\pm\mp}^{p_1 p_2} &= \frac{e^{\pi\kappa(k_s)}}{2\pi^2} H^2 [\cosh(2\pi\kappa(k_s)) + \cosh(2\pi\mu)] e^{\mp i\pi(p_1-p_2)/2} \\ &\times \left[G_{\mp i\kappa(k_s),\mu}^{p_1}(u_1) u_1^{i\mu} + G_{\mp i\kappa(k_s),-\mu}^{p_1}(u_1) u_1^{-i\mu} \right] \left[G_{\pm i\kappa(k_s),\mu}^{p_2}(u_2) u_2^{i\mu} + G_{\pm i\kappa(k_s),-\mu}^{p_2}(u_2) u_2^{-i\mu} \right], \end{aligned} \quad (\text{A.10})$$

where

$$G_{\pm i\kappa(k_s),\mu}^p(u) \equiv i\pi \operatorname{csch}(2\pi\mu) \left(\frac{u}{2} \right)^{5/2+p} {}_2F_1 \left[\begin{matrix} \frac{5}{2} + p + i\mu, \frac{1}{2} + i\mu \pm i\kappa(k_s) \\ 1 + 2i\mu \end{matrix} \middle| u \right]. \quad (\text{A.11})$$

In particular, in the hierarchical collapsed limit $u_1 \ll u_2 \ll 1$, we obtain

$$\lim_{u_1 \ll u_2 \ll 1} \mathcal{I}_{\pm\mp}^{p_1 p_2} = \sum_{a,b=\pm} \tilde{\mathcal{C}}_{\pm\mp|ab} \tilde{\mathcal{U}}_{\pm|a}^{p_1}(u_1) \tilde{\mathcal{U}}_{\mp|b}^{p_2}(u_2), \quad (\text{A.12})$$

where

$$\tilde{\mathcal{C}}_{\pm\mp|++} = \tilde{\mathcal{C}}_{\pm\mp|+-} = \tilde{\mathcal{C}}_{\pm\mp|-+} = \tilde{\mathcal{C}}_{\pm\mp|--} = \frac{e^{\pi\kappa}}{2\pi^2} H^2 [\cosh(2\pi\kappa(k_s)) + \cosh(2\pi\mu)] e^{\mp i\pi(p_1-p_2)/2}, \quad (\text{A.13})$$

and

$$\tilde{\mathcal{U}}_{a|b}^p(u) = iab 2^{iab\mu} \pi \operatorname{csch}(2\pi\mu) \left(\frac{u}{2} \right)^{5/2+p+iab\mu} \Gamma \left[\begin{matrix} \frac{5}{2} + p + iab\mu, \frac{1}{2} - ia\kappa + iab\mu \\ 1 + 2iab\mu \end{matrix} \right]. \quad (\text{A.14})$$

Same sign seed $\mathcal{I}_{\pm\pm}^{p_1 p_2}$

For the same sign seed integral, we adopt a division of the propagators in the same way employed in [128, 132],

$$D_{\pm\pm}(k; \tau_1, \tau_2) = D_{\geq}(k; \tau_1, \tau_2) + [D_{\leq}(k; \tau_1, \tau_2) - D_{\geq}(k; \tau_1, \tau_2)] \theta(\tau_2 - \tau_1), \quad (\text{A.15})$$

and accordingly, we define

$$\mathcal{I}_{\pm\pm}^{p_1 p_2} = \mathcal{I}_{\pm\pm,F,>}^{p_1 p_2} + \mathcal{I}_{\pm\pm,TO,>}^{p_1 p_2}, \quad (r_1 < r_2) \quad (\text{A.16})$$

where the factorized (F) integral $\mathcal{I}_{\pm\pm,F,>}^{p_1 p_2}$ and the time-ordered (TO) integral $\mathcal{I}_{\pm\pm,TO,>}^{p_1 p_2}$ are expressed as

$$\mathcal{I}_{\pm\pm,F,>}^{p_1 p_2} = -k_s^{5+p_{12}} \int_{-\infty}^0 d\tau_1 d\tau_2 (-\tau_1)^{p_1} (-\tau_2)^{p_2} e^{\pm i(k_{12}\tau_1 + k_{34}\tau_2)} D_{\geq}(k_s; \tau_1, \tau_2), \quad (\text{A.17})$$

$$\begin{aligned} \mathcal{I}_{\pm\pm,TO,>}^{p_1 p_2} &= -k_s^{5+p_{12}} \int_{-\infty}^0 d\tau_2 \int_{-\infty}^{\tau_2} d\tau_1 (-\tau_1)^{p_1} (-\tau_2)^{p_2} e^{\pm i(k_{12}\tau_1 + k_{34}\tau_2)} \\ &\times [D_{\leq}(k_s; \tau_1, \tau_2) - D_{\geq}(k_s; \tau_1, \tau_2)]. \end{aligned} \quad (\text{A.18})$$

Let us start from the factorized (F) integral $\mathcal{I}_{\pm\pm, \text{F}, >}$. We rewrite the propagators $D_{\pm\mp}$ using the Mellin–Barnes representations Eqs. (A.1) and (A.2):

$$\begin{aligned} D_{\pm\mp}(k; \tau_1, \tau_2) &= \frac{e^{\pi\kappa} H^2}{\pi\Gamma\left[\frac{1}{2} - i\mu \pm i\kappa, \frac{1}{2} + i\mu \pm i\kappa\right]} e^{\mp i\kappa(\tau_1 + \tau_2)} \\ &\times \int_{-i\infty}^{i\infty} \frac{ds_1}{2\pi i} \frac{ds_2}{2\pi i} e^{\mp i\pi(s_1 - s_2)/2} \cos\pi(s_1 \mp i\kappa) (2k)^{-s_{12}} (-\tau_1)^{-s_1+3/2} (-\tau_2)^{-s_2+3/2} \\ &\times \Gamma\left[-s_1 + \frac{1}{2} \pm i\kappa, -s_2 + \frac{1}{2} \pm i\kappa, s_1 - i\mu, s_1 + i\mu, s_2 - i\mu, s_2 + i\mu\right], \end{aligned} \quad (\text{A.19})$$

which leads to the subsequent expression of $\mathcal{I}_{\pm\pm, \text{F}, >}$ after the τ_i -integration,

$$\begin{aligned} \mathcal{I}_{\pm\pm, \text{F}, >}^{p_1 p_2} &= \frac{\pm i e^{\pi\kappa(k_s)} H^2}{\pi\Gamma\left[\frac{1}{2} - i\mu \mp i\kappa(k_s), \frac{1}{2} + i\mu \mp i\kappa(k_s)\right]} \left(\frac{u_1}{2}\right)^{5/2+p_1} \left(\frac{u_2}{2}\right)^{5/2+p_2} e^{\mp i\pi(p_1+p_2)/2} \\ &\times \int_{-i\infty}^{i\infty} \frac{ds_1}{2\pi i} \frac{ds_2}{2\pi i} e^{\pm i\pi s_1} \cos\pi(s_1 \pm i\kappa(k_s)) u_1^{-s_1} u_2^{-s_2} \Gamma\left[p_1 + \frac{5}{2} - s_1, p_2 + \frac{5}{2} - s_2\right] \\ &\times \Gamma\left[-s_1 + \frac{1}{2} \mp i\kappa(k_s), -s_2 + \frac{1}{2} \mp i\kappa(k_s), s_1 - i\mu, s_1 + i\mu, s_2 - i\mu, s_2 + i\mu\right]. \end{aligned} \quad (\text{A.20})$$

The integration over s_i and the summation of the residues can be executed following a similar procedure, and we obtain

$$\begin{aligned} \mathcal{I}_{\pm\pm, \text{F}, >}^{p_1 p_2} &= \frac{\pm i e^{\pi\kappa(k_s)} H^2}{\pi\Gamma\left[\frac{1}{2} - i\mu \mp i\kappa(k_s), \frac{1}{2} + i\mu \mp i\kappa(k_s)\right]} \left(\frac{u_1}{2}\right)^{5/2+p_1} \left(\frac{u_2}{2}\right)^{5/2+p_2} e^{\mp i\pi(p_1+p_2)/2} \\ &\times \sum_{n_1=0}^{\infty} \left\{ \frac{(-1)^{n_1}}{n_1!} e^{\mp i\pi(n_1+i\mu)} \cos\pi(-n_1 - i\mu \pm i\kappa(k_s)) u_1^{n_1+i\mu} \right. \\ &\times \Gamma\left[-n_1 - 2i\mu, n_1 + i\mu + \frac{1}{2} \mp i\kappa(k_s), n_1 + i\mu + p_1 + \frac{5}{2}\right] + (\mu \rightarrow -\mu) \Big\} \\ &\times \sum_{n_2=0}^{\infty} \left\{ \frac{(-1)^{n_2}}{n_2!} u_2^{n_2+i\mu} \Gamma\left[-n_2 - 2i\mu, n_2 + i\mu + \frac{1}{2} \mp i\kappa(k_s), n_2 + i\mu + p_2 + \frac{5}{2}\right] + (\mu \rightarrow -\mu) \right\} \end{aligned} \quad (\text{A.21})$$

$$\begin{aligned} &= \frac{\pm i e^{\pi\kappa(k_s)} H^2}{\pi\Gamma\left[\frac{1}{2} - i\mu \mp i\kappa(k_s), \frac{1}{2} + i\mu \mp i\kappa(k_s)\right]} e^{\mp i\pi(p_1+p_2)/2} \\ &\times \left[e^{\pm\pi\mu} \cosh\pi(\mu \mp \kappa(k_s)) G_{\mp i\kappa(k_s), \mu}^{p_1}(u_1) u_1^{i\mu} + e^{\mp\pi\mu} \cosh\pi(\mu \pm \kappa(k_s)) G_{\mp i\kappa(k_s), -\mu}^{p_1}(u_1) u_1^{-i\mu} \right] \\ &\times \left[G_{\mp i\kappa(k_s), \mu}^{p_2}(u_2) u_2^{i\mu} + G_{\mp i\kappa(k_s), -\mu}^{p_2}(u_2) u_2^{-i\mu} \right], \end{aligned} \quad (\text{A.22})$$

where the G -function is defined in Eq. (A.11).

In the same manner, The time-ordered (TO) integral $\mathcal{I}_{\pm\pm,\text{TO},>}^{p_1 p_2}$ can be transformed to

$$\begin{aligned} \mathcal{I}_{++,\text{TO},>}^{p_1 p_2} &= \frac{i e^{\pi \kappa(k_s)} H^2}{\pi \Gamma \left[\frac{1}{2} - i\mu - i\kappa(k_s), \frac{1}{2} + i\mu - i\kappa(k_s) \right]} \frac{e^{-i\pi(p_1+p_2)/2}}{2^{5+p_1+p_2}} \int_{-i\infty}^{+i\infty} \frac{ds_1}{2\pi i} \frac{ds_2}{2\pi i} \\ &\times \left[e^{i\pi s_2} \cos \pi(s_2 + i\kappa(k_s)) - e^{i\pi s_1} \cos \pi(s_1 + i\kappa(k_s)) \right] u_1^{-s_{12}+5+p_1+p_2} \\ &\times \Gamma \left[-s_1 + \frac{1}{2} - i\kappa(k_s), -s_2 + \frac{1}{2} - i\kappa(k_s), s_1 - i\mu, s_1 + i\mu, s_2 - i\mu, s_2 + i\mu \right] \\ &\times {}_2\mathcal{F}_1 \left[\begin{matrix} p_2 + \frac{5}{2} - s_2, p_1 + p_2 + 5 - s_{12} \\ p_2 + \frac{7}{2} - s_2 \end{matrix} \middle| -\frac{u_1}{u_2} \right] \end{aligned} \quad (\text{A.23})$$

by utilizing Eq. (A.19) and the integration formula

$$\begin{aligned} &\int_{-\infty}^0 d\tau_2 \int_{-\infty}^{\tau_2} d\tau_1 e^{\pm(i\kappa_{12}\tau_1 + i\kappa_{34}\tau_2)} (-\tau_1)^{p-1} (-\tau_2)^{q-1} \\ &= e^{\mp i(p+q)\frac{\pi}{2}} k_{12}^{-p-q} {}_2\mathcal{F}_1 \left[\begin{matrix} q, p+q \\ 1+q \end{matrix} \middle| -\frac{k_{34}}{k_{12}} \right]. \end{aligned} \quad (\text{A.24})$$

Subsequently, the complex s_i -integral leads to

$$\begin{aligned} \mathcal{I}_{++,\text{TO},>}^{p_1 p_2} &= \frac{i H^2 e^{-i\pi(p_1+p_2)/2}}{2^{5+p_1+p_2}} \sum_{n_1, n_2=0}^{\infty} \frac{(-1)^{n_{12}}}{n_1! n_2!} u_1^{n_{12}+5+p_1+p_2} \\ &\times \left\{ \frac{1}{2\mu} \left(\frac{1}{2} - i\mu - i\kappa(k_s) \right)_{n_1} \left(\frac{1}{2} + i\mu - i\kappa(k_s) \right)_{n_2} (2i\mu)_{-n_1} (-2i\mu)_{-n_2} \right. \\ &\times {}_2\mathcal{F}_1 \left[\begin{matrix} n_2 + p_2 + \frac{5}{2} + i\mu, n_{12} + p_1 + p_2 + 5 \\ n_2 + p_2 + \frac{7}{2} + i\mu \end{matrix} \middle| -\frac{u_1}{u_2} \right] + (\mu \rightarrow -\mu) \Big\}, \end{aligned} \quad (\text{A.25})$$

where $(z)_n \equiv \Gamma[z+n]/\Gamma[z]$ denotes the Pochhammer symbol. The minus sign seed $\mathcal{I}_{--,\text{TO},>}^{p_1 p_2}$ is obtained by taking a conjugate of Eq. (A.25). In contrast to the previous cases, performing the double summation presented above poses technical challenges.

The hierarchical collapsed limit ($u_1 \ll u_2 \ll 1$) of $\mathcal{I}_{\pm\pm}^{p_1 p_2}$ enables us to determine the integration constants appearing in Section 3. Under the limit, the dominant contribution comes from the poles with $n_{1,2} = 0$ in Eqs. (A.21) and (A.25). Additionally, $\mathcal{I}_{++,\text{TO},>}^{p_1 p_2}$ is subdominant in comparison to $\mathcal{I}_{\pm\pm,\text{F},>}^{p_1 p_2}$. Combining these evaluations, we obtain

$$\lim_{u_1 \ll u_2 \ll 1} \mathcal{I}_{\pm\pm}^{p_1 p_2} = \sum_{a,b=\pm} \tilde{\mathcal{C}}_{\pm\pm|ab} \tilde{\mathcal{U}}_{\pm|a}^{p_1}(u_1) \tilde{\mathcal{U}}_{\pm|b}^{p_2}(u_2), \quad (\text{A.26})$$

where

$$\tilde{\mathcal{C}}_{\pm\pm|++} = \tilde{\mathcal{C}}_{\pm\pm|+-} = \frac{\pm i e^{\pi(\kappa(k_s)+\mu)} \cosh \pi(-\mu + \kappa(k_s)) H^2}{\pi \Gamma \left[\frac{1}{2} - i\mu \mp i\kappa(k_s), \frac{1}{2} + i\mu \mp i\kappa(k_s) \right]} e^{\mp i\pi(p_1+p_2)/2}, \quad (\text{A.27})$$

$$\tilde{\mathcal{C}}_{\pm\pm|-+} = \tilde{\mathcal{C}}_{\pm\pm|--} = \frac{\pm i e^{\pi(\kappa(k_s)-\mu)} \cosh \pi(\mu + \kappa(k_s)) H^2}{\pi \Gamma \left[\frac{1}{2} - i\mu \mp i\kappa(k_s), \frac{1}{2} + i\mu \mp i\kappa(k_s) \right]} e^{\mp i\pi(p_1+p_2)/2}. \quad (\text{A.28})$$

Note that we confirmed that our outcomes (A.7), (A.22), and (A.25) are consistent with the constant mass results of Refs. [128, 132] in the limit $\kappa \rightarrow 0$, as described in the following appendix in detail.

B Constant Mass Limit

In case where the coupling (2.1) is constant, $g(\phi) = m_0^2$, which corresponds to $\kappa \rightarrow 0$, the seed integrals with single soft limit, Eqs. (3.53) and (3.54), should reproduce the results for the constant mass scenario presented in Ref. [128, 132]. Since the mode function of the massive field σ for the constant mass is expressed by the Hankel function (see Eq. (2.18)) whereas our case is the Whittaker function (see Eq. (2.17)), this limit provides a non-trivial consistency check.

In the subsequent discussion, we frequently use the following formulae for the Gamma function:

$$\Gamma(-z)\Gamma(z+1) = -\frac{\pi}{\sin \pi z}, \quad (\text{B.1})$$

$$\Gamma(2z) = \frac{2^{2z-1}}{\sqrt{\pi}} \Gamma(z) \Gamma\left(z + \frac{1}{z}\right). \quad (\text{B.2})$$

In the limit $\kappa \rightarrow 0$, Eqs. (3.53) and (3.54) are reduced to

$$\mathcal{I}_{\pm\mp}^{p_1 p_2}(u_1, 1, v(k_3))/H^2 = \frac{e^{\mp i \frac{\pi}{2} \bar{p}_{12}}}{2^{7/2+p_2} \pi^{1/2}} \Gamma\left[\begin{matrix} \frac{5}{2} + p_2 - i\mu, \frac{5}{2} + p_2 + i\mu \\ 3 + p_2 \end{matrix}\right] [\mathcal{Y}_+^{p_1}(u) + \mathcal{Y}_-^{p_1}(u)], \quad (\text{B.3})$$

$$\begin{aligned} \mathcal{I}_{\pm\pm}^{p_1 p_2}(u_1, 1, v(k_3))/H^2 &= \frac{e^{\mp i \frac{\pi}{2} p_{12}} \Gamma(5 + p_{12}) u_1^{5+p_{12}}}{2^{5+p_{12}} \left[\left(\frac{5}{2} + p_2\right)^2 + \mu^2\right]} {}_3F_2\left[\begin{matrix} 1, 3 + p_2, 5 + p_{12} \\ \frac{7}{2} + p_2 - i\mu, \frac{7}{2} + p_2 + i\mu \end{matrix} \middle| u_1\right] \\ &+ \frac{\pm i e^{\mp i \frac{\pi}{2} p_{12}}}{2^{7/2+p_2} \pi^{1/2}} \Gamma\left[\begin{matrix} \frac{5}{2} + p_2 - i\mu, \frac{5}{2} + p_2 + i\mu \\ 3 + p_2 \end{matrix}\right] [e^{\pi\mu} \mathcal{Y}_{\pm}^{p_1}(u_1) + e^{-\pi\mu} \mathcal{Y}_{\mp}^{p_1}(u_1)], \end{aligned} \quad (\text{B.4})$$

respectively, where

$$\mathcal{Y}_{\pm}^p(u) \equiv 2^{\mp i\mu} \left(\frac{u}{2}\right)^{5/2+p \pm i\mu} \Gamma\left[\begin{matrix} 5 \\ \frac{5}{2} + p \pm i\mu, \mp i\mu \end{matrix}\right] {}_2F_1\left[\begin{matrix} \frac{5}{2} + p \pm i\mu, \frac{1}{2} \pm i\mu \\ 1 \pm 2i\mu \end{matrix} \middle| u\right]. \quad (\text{B.5})$$

These equations are in agreement with the results of Ref. [132].

In the same way, for the seed integrals with double soft limit (Eqs. (3.59) and (3.60)), we can express them in the limit $\kappa \rightarrow 0$ as follows:

$$\mathcal{I}_{\pm\mp}^{p_1 p_2}(1, 1, v(k_3))/H^2 = \frac{e^{\mp i \frac{\pi}{2} \bar{p}_{12}}}{2^{5+p_{12}}} \Gamma\left[\begin{matrix} \frac{5}{2} + p_1 - i\mu, \frac{5}{2} + p_1 + i\mu, \frac{5}{2} + p_2 - i\mu, \frac{5}{2} + p_2 + i\mu \\ 3 + p_1, 3 + p_2 \end{matrix}\right], \quad (\text{B.6})$$

and

$$\begin{aligned}
& \mathcal{I}_{\pm\pm}^{p_1 p_2}(1, 1, v(k_3))/H^2 \\
&= \frac{\pm i e^{\mp i \frac{\pi}{2} p_{12}} e^{-\pi \mu}}{2^{5+p_{12}}} \Gamma \left[\begin{matrix} \frac{5}{2} + p_1 - i\mu, \frac{5}{2} + p_1 + i\mu, \frac{5}{2} + p_2 - i\mu, \frac{5}{2} + p_2 + i\mu \\ 3 + p_1, 3 + p_2 \end{matrix} \right] \\
&- \frac{e^{\mp i \frac{\pi}{2} p_{12}}}{2^{p_{12}+5}} \Gamma \left[\begin{matrix} \frac{5}{2} + p_2 \pm i\mu, \frac{5}{2} + p_1 \pm i\mu \\ \frac{1}{2} \pm i\mu \end{matrix} \right] {}_3\mathcal{F}_2 \left[\begin{matrix} \frac{1}{2} \pm i\mu, 5 + p_{12}, 1 \\ \frac{7}{2} + p_1 \pm i\mu, \frac{7}{2} + p_2 \pm i\mu \end{matrix} \middle| 1 \right]. \quad (\text{B.7})
\end{aligned}$$

Again, these expressions are consistent with the results of Ref. [132].

References

- [1] A. H. Jaffe et al. “Cosmology from MAXIMA-1, BOOMERANG and COBE / DMR CMB observations.” *Phys. Rev. Lett.* 86 (2001), pp. 3475–3479. DOI: [10.1103/PhysRevLett.86.3475](https://doi.org/10.1103/PhysRevLett.86.3475). arXiv: [astro-ph/0007333](https://arxiv.org/abs/astro-ph/0007333).
- [2] C. L. Bennett et al. “Nine-Year Wilkinson Microwave Anisotropy Probe (WMAP) Observations: Final Maps and Results.” *Astrophys. J. Suppl.* 208 (2013), p. 20. DOI: [10.1088/0067-0049/208/2/20](https://doi.org/10.1088/0067-0049/208/2/20). arXiv: [1212.5225](https://arxiv.org/abs/1212.5225) [[astro-ph.CO](https://arxiv.org/abs/astro-ph)].
- [3] Y. Akrami et al. “Planck 2018 results. X. Constraints on inflation.” *Astron. Astrophys.* 641 (2020), A10. DOI: [10.1051/0004-6361/201833887](https://doi.org/10.1051/0004-6361/201833887). arXiv: [1807.06211](https://arxiv.org/abs/1807.06211) [[astro-ph.CO](https://arxiv.org/abs/astro-ph)].
- [4] A. A. Starobinsky. “A New Type of Isotropic Cosmological Models Without Singularity.” *Phys. Lett. B* 91 (1980). Ed. by I. M. Khalatnikov and V. P. Mineev, pp. 99–102. DOI: [10.1016/0370-2693\(80\)90670-X](https://doi.org/10.1016/0370-2693(80)90670-X).
- [5] K. Sato. “First Order Phase Transition of a Vacuum and Expansion of the Universe.” *Mon. Not. Roy. Astron. Soc.* 195 (1981), pp. 467–479.
- [6] A. H. Guth. “The Inflationary Universe: A Possible Solution to the Horizon and Flatness Problems.” *Phys. Rev. D* 23 (1981). Ed. by L.-Z. Fang and R. Ruffini, pp. 347–356. DOI: [10.1103/PhysRevD.23.347](https://doi.org/10.1103/PhysRevD.23.347).
- [7] A. D. Linde. “A New Inflationary Universe Scenario: A Possible Solution of the Horizon, Flatness, Homogeneity, Isotropy and Primordial Monopole Problems.” *Phys. Lett. B* 108 (1982). Ed. by L.-Z. Fang and R. Ruffini, pp. 389–393. DOI: [10.1016/0370-2693\(82\)91219-9](https://doi.org/10.1016/0370-2693(82)91219-9).
- [8] A. Albrecht and P. J. Steinhardt. “Cosmology for Grand Unified Theories with Radiatively Induced Symmetry Breaking.” *Phys. Rev. Lett.* 48 (1982). Ed. by L.-Z. Fang and R. Ruffini, pp. 1220–1223. DOI: [10.1103/PhysRevLett.48.1220](https://doi.org/10.1103/PhysRevLett.48.1220).
- [9] X. Chen and Y. Wang. “Quasi-Single Field Inflation and Non-Gaussianities.” *JCAP* 04 (2010), p. 027. DOI: [10.1088/1475-7516/2010/04/027](https://doi.org/10.1088/1475-7516/2010/04/027). arXiv: [0911.3380](https://arxiv.org/abs/0911.3380) [[hep-th](https://arxiv.org/abs/hep-th)].

- [10] D. Baumann and D. Green. “Signatures of Supersymmetry from the Early Universe.” *Phys. Rev. D* 85 (2012), p. 103520. DOI: [10.1103/PhysRevD.85.103520](https://doi.org/10.1103/PhysRevD.85.103520). arXiv: [1109.0292](https://arxiv.org/abs/1109.0292) [hep-th].
- [11] T. Noumi, M. Yamaguchi, and D. Yokoyama. “Effective field theory approach to quasi-single field inflation and effects of heavy fields.” *JHEP* 06 (2013), p. 051. DOI: [10.1007/JHEP06\(2013\)051](https://doi.org/10.1007/JHEP06(2013)051). arXiv: [1211.1624](https://arxiv.org/abs/1211.1624) [hep-th].
- [12] N. Arkani-Hamed and J. Maldacena. “Cosmological Collider Physics.” (2015). arXiv: [1503.08043](https://arxiv.org/abs/1503.08043) [hep-th].
- [13] X. Chen and Y. Wang. “Large non-Gaussianities with Intermediate Shapes from Quasi-Single Field Inflation.” *Phys. Rev. D* 81 (2010), p. 063511. DOI: [10.1103/PhysRevD.81.063511](https://doi.org/10.1103/PhysRevD.81.063511). arXiv: [0909.0496](https://arxiv.org/abs/0909.0496) [astro-ph.CO].
- [14] V. Assassi, D. Baumann, and D. Green. “On Soft Limits of Inflationary Correlation Functions.” *JCAP* 11 (2012), p. 047. DOI: [10.1088/1475-7516/2012/11/047](https://doi.org/10.1088/1475-7516/2012/11/047). arXiv: [1204.4207](https://arxiv.org/abs/1204.4207) [hep-th].
- [15] E. Sefusatti et al. “Effects and Detectability of Quasi-Single Field Inflation in the Large-Scale Structure and Cosmic Microwave Background.” *JCAP* 08 (2012), p. 033. DOI: [10.1088/1475-7516/2012/08/033](https://doi.org/10.1088/1475-7516/2012/08/033). arXiv: [1204.6318](https://arxiv.org/abs/1204.6318) [astro-ph.CO].
- [16] J. Norena et al. “Prospects for constraining the shape of non-Gaussianity with the scale-dependent bias.” *JCAP* 08 (2012), p. 019. DOI: [10.1088/1475-7516/2012/08/019](https://doi.org/10.1088/1475-7516/2012/08/019). arXiv: [1204.6324](https://arxiv.org/abs/1204.6324) [astro-ph.CO].
- [17] X. Chen and Y. Wang. “Quasi-Single Field Inflation with Large Mass.” *JCAP* 09 (2012), p. 021. DOI: [10.1088/1475-7516/2012/09/021](https://doi.org/10.1088/1475-7516/2012/09/021). arXiv: [1205.0160](https://arxiv.org/abs/1205.0160) [hep-th].
- [18] S. Pi and M. Sasaki. “Curvature Perturbation Spectrum in Two-field Inflation with a Turning Trajectory.” *JCAP* 10 (2012), p. 051. DOI: [10.1088/1475-7516/2012/10/051](https://doi.org/10.1088/1475-7516/2012/10/051). arXiv: [1205.0161](https://arxiv.org/abs/1205.0161) [hep-th].
- [19] S. C  spedes and G. A. Palma. “Cosmic inflation in a landscape of heavy-fields.” *JCAP* 10 (2013), p. 051. DOI: [10.1088/1475-7516/2013/10/051](https://doi.org/10.1088/1475-7516/2013/10/051). arXiv: [1303.4703](https://arxiv.org/abs/1303.4703) [hep-th].
- [20] J.-O. Gong, S. Pi, and M. Sasaki. “Equilateral non-Gaussianity from heavy fields.” *JCAP* 11 (2013), p. 043. DOI: [10.1088/1475-7516/2013/11/043](https://doi.org/10.1088/1475-7516/2013/11/043). arXiv: [1306.3691](https://arxiv.org/abs/1306.3691) [hep-th].
- [21] R. Emami. “Spectroscopy of Masses and Couplings during Inflation.” *JCAP* 04 (2014), p. 031. DOI: [10.1088/1475-7516/2014/04/031](https://doi.org/10.1088/1475-7516/2014/04/031). arXiv: [1311.0184](https://arxiv.org/abs/1311.0184) [hep-th].
- [22] A. Kehagias and A. Riotto. “High Energy Physics Signatures from Inflation and Conformal Symmetry of de Sitter.” *Fortsch. Phys.* 63 (2015), pp. 531–542. DOI: [10.1002/prop.201500025](https://doi.org/10.1002/prop.201500025). arXiv: [1501.03515](https://arxiv.org/abs/1501.03515) [hep-th].

- [23] J. Liu, Y. Wang, and S. Zhou. “Inflation with Massive Vector Fields.” *JCAP* 08 (2015), p. 033. DOI: [10.1088/1475-7516/2015/08/033](#). arXiv: [1502.05138 \[hep-th\]](#).
- [24] E. Dimastrogiovanni, M. Fasiello, and M. Kamionkowski. “Imprints of Massive Primordial Fields on Large-Scale Structure.” *JCAP* 02 (2016), p. 017. DOI: [10.1088/1475-7516/2016/02/017](#). arXiv: [1504.05993 \[astro-ph.CO\]](#).
- [25] F. Schmidt, N. E. Chisari, and C. Dvorkin. “Imprint of inflation on galaxy shape correlations.” *JCAP* 10 (2015), p. 032. DOI: [10.1088/1475-7516/2015/10/032](#). arXiv: [1506.02671 \[astro-ph.CO\]](#).
- [26] X. Chen, M. H. Namjoo, and Y. Wang. “Quantum Primordial Standard Clocks.” *JCAP* 02 (2016), p. 013. DOI: [10.1088/1475-7516/2016/02/013](#). arXiv: [1509.03930 \[astro-ph.CO\]](#).
- [27] L. V. Delacretaz, T. Noumi, and L. Senatore. “Boost Breaking in the EFT of Inflation.” *JCAP* 02 (2017), p. 034. DOI: [10.1088/1475-7516/2017/02/034](#). arXiv: [1512.04100 \[hep-th\]](#).
- [28] B. Bonga et al. “Cosmic variance in inflation with two light scalars.” *JCAP* 05 (2016), p. 018. DOI: [10.1088/1475-7516/2016/05/018](#). arXiv: [1512.05365 \[astro-ph.CO\]](#).
- [29] X. Chen, Y. Wang, and Z.-Z. Xianyu. “Loop Corrections to Standard Model Fields in Inflation.” *JHEP* 08 (2016), p. 051. DOI: [10.1007/JHEP08\(2016\)051](#). arXiv: [1604.07841 \[hep-th\]](#).
- [30] R. Flauger et al. “Productive Interactions: heavy particles and non-Gaussianity.” *JCAP* 10 (2017), p. 058. DOI: [10.1088/1475-7516/2017/10/058](#). arXiv: [1606.00513 \[hep-th\]](#).
- [31] H. Lee, D. Baumann, and G. L. Pimentel. “Non-Gaussianity as a Particle Detector.” *JHEP* 12 (2016), p. 040. DOI: [10.1007/JHEP12\(2016\)040](#). arXiv: [1607.03735 \[hep-th\]](#).
- [32] L. V. Delacretaz, V. Gorbenko, and L. Senatore. “The Supersymmetric Effective Field Theory of Inflation.” *JHEP* 03 (2017), p. 063. DOI: [10.1007/JHEP03\(2017\)063](#). arXiv: [1610.04227 \[hep-th\]](#).
- [33] P. D. Meerburg et al. “Prospects for Cosmological Collider Physics.” *JCAP* 03 (2017), p. 050. DOI: [10.1088/1475-7516/2017/03/050](#). arXiv: [1610.06559 \[astro-ph.CO\]](#).
- [34] X. Chen, Y. Wang, and Z.-Z. Xianyu. “Standard Model Background of the Cosmological Collider.” *Phys. Rev. Lett.* 118.26 (2017), p. 261302. DOI: [10.1103/PhysRevLett.118.261302](#). arXiv: [1610.06597 \[hep-th\]](#).
- [35] X. Chen, Y. Wang, and Z.-Z. Xianyu. “Standard Model Mass Spectrum in Inflationary Universe.” *JHEP* 04 (2017), p. 058. DOI: [10.1007/JHEP04\(2017\)058](#). arXiv: [1612.08122 \[hep-th\]](#).

- [36] A. Kehagias and A. Riotto. “On the Inflationary Perturbations of Massive Higher-Spin Fields.” *JCAP* 07 (2017), p. 046. DOI: [10.1088/1475-7516/2017/07/046](https://doi.org/10.1088/1475-7516/2017/07/046). arXiv: [1705.05834](https://arxiv.org/abs/1705.05834) [[hep-th](#)].
- [37] H. An et al. “Quasi Single Field Inflation in the non-perturbative regime.” *JHEP* 06 (2018), p. 105. DOI: [10.1007/JHEP06\(2018\)105](https://doi.org/10.1007/JHEP06(2018)105). arXiv: [1706.09971](https://arxiv.org/abs/1706.09971) [[hep-ph](#)].
- [38] X. Tong, Y. Wang, and S. Zhou. “On the Effective Field Theory for Quasi-Single Field Inflation.” *JCAP* 11 (2017), p. 045. DOI: [10.1088/1475-7516/2017/11/045](https://doi.org/10.1088/1475-7516/2017/11/045). arXiv: [1708.01709](https://arxiv.org/abs/1708.01709) [[astro-ph.CO](#)].
- [39] A. V. Iyer et al. “Strongly Coupled Quasi-Single Field Inflation.” *JCAP* 01 (2018), p. 041. DOI: [10.1088/1475-7516/2018/01/041](https://doi.org/10.1088/1475-7516/2018/01/041). arXiv: [1710.03054](https://arxiv.org/abs/1710.03054) [[hep-th](#)].
- [40] H. An et al. “Non-Gaussian Enhancements of Galactic Halo Correlations in Quasi-Single Field Inflation.” *Phys. Rev. D* 97.12 (2018), p. 123528. DOI: [10.1103/PhysRevD.97.123528](https://doi.org/10.1103/PhysRevD.97.123528). arXiv: [1711.02667](https://arxiv.org/abs/1711.02667) [[hep-ph](#)].
- [41] S. Kumar and R. Sundrum. “Heavy-Lifting of Gauge Theories By Cosmic Inflation.” *JHEP* 05 (2018), p. 011. DOI: [10.1007/JHEP05\(2018\)011](https://doi.org/10.1007/JHEP05(2018)011). arXiv: [1711.03988](https://arxiv.org/abs/1711.03988) [[hep-ph](#)].
- [42] S. Riquelme M. “Non-Gaussianities in a two-field generalization of Natural Inflation.” *JCAP* 04 (2018), p. 027. DOI: [10.1088/1475-7516/2018/04/027](https://doi.org/10.1088/1475-7516/2018/04/027). arXiv: [1711.08549](https://arxiv.org/abs/1711.08549) [[astro-ph.CO](#)].
- [43] G. Franciolini, A. Kehagias, and A. Riotto. “Imprints of Spinning Particles on Primordial Cosmological Perturbations.” *JCAP* 02 (2018), p. 023. DOI: [10.1088/1475-7516/2018/02/023](https://doi.org/10.1088/1475-7516/2018/02/023). arXiv: [1712.06626](https://arxiv.org/abs/1712.06626) [[hep-th](#)].
- [44] X. Tong, Y. Wang, and S. Zhou. “Unsuppressed primordial standard clocks in warm quasi-single field inflation.” *JCAP* 06 (2018), p. 013. DOI: [10.1088/1475-7516/2018/06/013](https://doi.org/10.1088/1475-7516/2018/06/013). arXiv: [1801.05688](https://arxiv.org/abs/1801.05688) [[hep-th](#)].
- [45] X. Chen et al. “Quantum Standard Clocks in the Primordial Trispectrum.” *JCAP* 05 (2018), p. 049. DOI: [10.1088/1475-7516/2018/05/049](https://doi.org/10.1088/1475-7516/2018/05/049). arXiv: [1803.04412](https://arxiv.org/abs/1803.04412) [[hep-th](#)].
- [46] R. Saito and T. Kubota. “Heavy Particle Signatures in Cosmological Correlation Functions with Tensor Modes.” *JCAP* 06 (2018), p. 009. DOI: [10.1088/1475-7516/2018/06/009](https://doi.org/10.1088/1475-7516/2018/06/009). arXiv: [1804.06974](https://arxiv.org/abs/1804.06974) [[hep-th](#)].
- [47] G. Cabass, E. Pajer, and F. Schmidt. “Imprints of Oscillatory Bispectra on Galaxy Clustering.” *JCAP* 09 (2018), p. 003. DOI: [10.1088/1475-7516/2018/09/003](https://doi.org/10.1088/1475-7516/2018/09/003). arXiv: [1804.07295](https://arxiv.org/abs/1804.07295) [[astro-ph.CO](#)].
- [48] Y. Wang et al. “Hybrid Quasi-Single Field Inflation.” *JCAP* 07 (2018), p. 068. DOI: [10.1088/1475-7516/2018/07/068](https://doi.org/10.1088/1475-7516/2018/07/068). arXiv: [1804.07541](https://arxiv.org/abs/1804.07541) [[astro-ph.CO](#)].

- [49] X. Chen, Y. Wang, and Z.-Z. Xianyu. “Neutrino Signatures in Primordial Non-Gaussianities.” *JHEP* 09 (2018), p. 022. DOI: [10.1007/JHEP09\(2018\)022](https://doi.org/10.1007/JHEP09(2018)022). arXiv: [1805.02656](https://arxiv.org/abs/1805.02656) [[hep-ph](#)].
- [50] N. Bartolo et al. “Supergravity, α -attractors and primordial non-Gaussianity.” *JCAP* 10 (2018), p. 017. DOI: [10.1088/1475-7516/2018/10/017](https://doi.org/10.1088/1475-7516/2018/10/017). arXiv: [1805.04269](https://arxiv.org/abs/1805.04269) [[astro-ph.CO](#)].
- [51] E. Dimastrogiovanni, M. Fasiello, and G. Tasinato. “Probing the inflationary particle content: extra spin-2 field.” *JCAP* 08 (2018), p. 016. DOI: [10.1088/1475-7516/2018/08/016](https://doi.org/10.1088/1475-7516/2018/08/016). arXiv: [1806.00850](https://arxiv.org/abs/1806.00850) [[astro-ph.CO](#)].
- [52] L. Bordin et al. “Light Particles with Spin in Inflation.” *JCAP* 10 (2018), p. 013. DOI: [10.1088/1475-7516/2018/10/013](https://doi.org/10.1088/1475-7516/2018/10/013). arXiv: [1806.10587](https://arxiv.org/abs/1806.10587) [[hep-th](#)].
- [53] X. Chen, A. Loeb, and Z.-Z. Xianyu. “Unique Fingerprints of Alternatives to Inflation in the Primordial Power Spectrum.” *Phys. Rev. Lett.* 122.12 (2019), p. 121301. DOI: [10.1103/PhysRevLett.122.121301](https://doi.org/10.1103/PhysRevLett.122.121301). arXiv: [1809.02603](https://arxiv.org/abs/1809.02603) [[astro-ph.CO](#)].
- [54] A. Achúcarro et al. “Constraints on Holographic Multifield Inflation and Models Based on the Hamilton-Jacobi Formalism.” *Phys. Rev. Lett.* 122.19 (2019), p. 191301. DOI: [10.1103/PhysRevLett.122.191301](https://doi.org/10.1103/PhysRevLett.122.191301). arXiv: [1809.05341](https://arxiv.org/abs/1809.05341) [[hep-th](#)].
- [55] W. Z. Chua et al. “Imprints of Schwinger Effect on Primordial Spectra.” *JHEP* 04 (2019), p. 066. DOI: [10.1007/JHEP04\(2019\)066](https://doi.org/10.1007/JHEP04(2019)066). arXiv: [1810.09815](https://arxiv.org/abs/1810.09815) [[hep-th](#)].
- [56] S. Kumar and R. Sundrum. “Seeing Higher-Dimensional Grand Unification In Primordial Non-Gaussianities.” *JHEP* 04 (2019), p. 120. DOI: [10.1007/JHEP04\(2019\)120](https://doi.org/10.1007/JHEP04(2019)120). arXiv: [1811.11200](https://arxiv.org/abs/1811.11200) [[hep-ph](#)].
- [57] G. Goon et al. “Shapes of gravity: Tensor non-Gaussianity and massive spin-2 fields.” *JHEP* 10 (2019), p. 182. DOI: [10.1007/JHEP10\(2019\)182](https://doi.org/10.1007/JHEP10(2019)182). arXiv: [1812.07571](https://arxiv.org/abs/1812.07571) [[hep-th](#)].
- [58] Y.-P. Wu. “Higgs as heavy-lifted physics during inflation.” *JHEP* 04 (2019), p. 125. DOI: [10.1007/JHEP04\(2019\)125](https://doi.org/10.1007/JHEP04(2019)125). arXiv: [1812.10654](https://arxiv.org/abs/1812.10654) [[hep-ph](#)].
- [59] D. Anninos et al. “Cosmological Shapes of Higher-Spin Gravity.” *JCAP* 04 (2019), p. 045. DOI: [10.1088/1475-7516/2019/04/045](https://doi.org/10.1088/1475-7516/2019/04/045). arXiv: [1902.01251](https://arxiv.org/abs/1902.01251) [[hep-th](#)].
- [60] L. Li et al. “Gravitational Production of Superheavy Dark Matter and Associated Cosmological Signatures.” *JHEP* 07 (2019), p. 067. DOI: [10.1007/JHEP07\(2019\)067](https://doi.org/10.1007/JHEP07(2019)067). arXiv: [1903.08842](https://arxiv.org/abs/1903.08842) [[astro-ph.CO](#)].
- [61] M. McAneny and A. K. Ridgway. “New Shapes of Primordial Non-Gaussianity from Quasi-Single Field Inflation with Multiple Isocurvatons.” *Phys. Rev. D* 100.4 (2019), p. 043534. DOI: [10.1103/PhysRevD.100.043534](https://doi.org/10.1103/PhysRevD.100.043534). arXiv: [1903.11607](https://arxiv.org/abs/1903.11607) [[astro-ph.CO](#)].

- [62] S. Kim et al. “Heavy Spinning Particles from Signs of Primordial Non-Gaussianities: Beyond the Positivity Bounds.” *JHEP* 12 (2019), p. 107. DOI: [10.1007/JHEP12\(2019\)107](https://doi.org/10.1007/JHEP12(2019)107). arXiv: [1906.11840](https://arxiv.org/abs/1906.11840) [[hep-th](#)].
- [63] S. Alexander et al. “Higher Spin Supersymmetry at the Cosmological Collider: Sculpting SUSY Ripples in the CMB.” *JHEP* 10 (2019), p. 156. DOI: [10.1007/JHEP10\(2019\)156](https://doi.org/10.1007/JHEP10(2019)156). arXiv: [1907.05829](https://arxiv.org/abs/1907.05829) [[hep-th](#)].
- [64] S. Lu, Y. Wang, and Z.-Z. Xianyu. “A Cosmological Higgs Collider.” *JHEP* 02 (2020), p. 011. DOI: [10.1007/JHEP02\(2020\)011](https://doi.org/10.1007/JHEP02(2020)011). arXiv: [1907.07390](https://arxiv.org/abs/1907.07390) [[hep-th](#)].
- [65] A. Hook, J. Huang, and D. Racco. “Searches for other vacua. Part II. A new Higgstory at the cosmological collider.” *JHEP* 01 (2020), p. 105. DOI: [10.1007/JHEP01\(2020\)105](https://doi.org/10.1007/JHEP01(2020)105). arXiv: [1907.10624](https://arxiv.org/abs/1907.10624) [[hep-ph](#)].
- [66] A. Hook, J. Huang, and D. Racco. “Minimal signatures of the Standard Model in non-Gaussianities.” *Phys. Rev. D* 101.2 (2020), p. 023519. DOI: [10.1103/PhysRevD.101.023519](https://doi.org/10.1103/PhysRevD.101.023519). arXiv: [1908.00019](https://arxiv.org/abs/1908.00019) [[hep-ph](#)].
- [67] S. Kumar and R. Sundrum. “Cosmological Collider Physics and the Curvaton.” *JHEP* 04 (2020), p. 077. DOI: [10.1007/JHEP04\(2020\)077](https://doi.org/10.1007/JHEP04(2020)077). arXiv: [1908.11378](https://arxiv.org/abs/1908.11378) [[hep-ph](#)].
- [68] T. Liu et al. “Probing P and CP Violations on the Cosmological Collider.” *JHEP* 04 (2020), p. 189. DOI: [10.1007/JHEP04\(2020\)189](https://doi.org/10.1007/JHEP04(2020)189). arXiv: [1909.01819](https://arxiv.org/abs/1909.01819) [[hep-ph](#)].
- [69] L.-T. Wang and Z.-Z. Xianyu. “In Search of Large Signals at the Cosmological Collider.” *JHEP* 02 (2020), p. 044. DOI: [10.1007/JHEP02\(2020\)044](https://doi.org/10.1007/JHEP02(2020)044). arXiv: [1910.12876](https://arxiv.org/abs/1910.12876) [[hep-ph](#)].
- [70] D.-G. Wang. “On the inflationary massive field with a curved field manifold.” *JCAP* 01 (2020), p. 046. DOI: [10.1088/1475-7516/2020/01/046](https://doi.org/10.1088/1475-7516/2020/01/046). arXiv: [1911.04459](https://arxiv.org/abs/1911.04459) [[astro-ph.CO](#)].
- [71] Y. Wang and Y. Zhu. “Cosmological Collider Signatures of Massive Vectors from Non-Gaussian Gravitational Waves.” *JCAP* 04 (2020), p. 049. DOI: [10.1088/1475-7516/2020/04/049](https://doi.org/10.1088/1475-7516/2020/04/049). arXiv: [2001.03879](https://arxiv.org/abs/2001.03879) [[astro-ph.CO](#)].
- [72] L. Li et al. “Cosmological Signatures of Superheavy Dark Matter.” *JHEP* 07 (2020), p. 231. DOI: [10.1007/JHEP07\(2020\)231](https://doi.org/10.1007/JHEP07(2020)231). arXiv: [2002.01131](https://arxiv.org/abs/2002.01131) [[hep-ph](#)].
- [73] L.-T. Wang and Z.-Z. Xianyu. “Gauge Boson Signals at the Cosmological Collider.” *JHEP* 11 (2020), p. 082. DOI: [10.1007/JHEP11\(2020\)082](https://doi.org/10.1007/JHEP11(2020)082). arXiv: [2004.02887](https://arxiv.org/abs/2004.02887) [[hep-ph](#)].
- [74] J. Fan and Z.-Z. Xianyu. “A Cosmic Microscope for the Preheating Era.” *JHEP* 01 (2021), p. 021. DOI: [10.1007/JHEP01\(2021\)021](https://doi.org/10.1007/JHEP01(2021)021). arXiv: [2005.12278](https://arxiv.org/abs/2005.12278) [[hep-ph](#)].
- [75] A. Bodas, S. Kumar, and R. Sundrum. “The Scalar Chemical Potential in Cosmological Collider Physics.” *JHEP* 02 (2021), p. 079. DOI: [10.1007/JHEP02\(2021\)079](https://doi.org/10.1007/JHEP02(2021)079). arXiv: [2010.04727](https://arxiv.org/abs/2010.04727) [[hep-ph](#)].

- [76] S. Aoki and M. Yamaguchi. “Disentangling mass spectra of multiple fields in cosmological collider.” *JHEP* 04 (2021), p. 127. DOI: [10.1007/JHEP04\(2021\)127](https://doi.org/10.1007/JHEP04(2021)127). arXiv: [2012.13667](https://arxiv.org/abs/2012.13667) [[hep-th](#)].
- [77] N. Maru and A. Okawa. “Non-Gaussianity from X, Y gauge bosons in Cosmological Collider Physics.” (2021). arXiv: [2101.10634](https://arxiv.org/abs/2101.10634) [[hep-ph](#)].
- [78] S. Kim et al. “Perturbative unitarity in quasi-single field inflation.” *JHEP* 07 (2021), p. 018. DOI: [10.1007/JHEP07\(2021\)018](https://doi.org/10.1007/JHEP07(2021)018). arXiv: [2102.04101](https://arxiv.org/abs/2102.04101) [[hep-th](#)].
- [79] S. Lu. “Axion isocurvature collider.” *JHEP* 04 (2022), p. 157. DOI: [10.1007/JHEP04\(2022\)157](https://doi.org/10.1007/JHEP04(2022)157). arXiv: [2103.05958](https://arxiv.org/abs/2103.05958) [[hep-th](#)].
- [80] C. M. Sou, X. Tong, and Y. Wang. “Chemical-potential-assisted particle production in FRW spacetimes.” *JHEP* 06 (2021), p. 129. DOI: [10.1007/JHEP06\(2021\)129](https://doi.org/10.1007/JHEP06(2021)129). arXiv: [2104.08772](https://arxiv.org/abs/2104.08772) [[hep-th](#)].
- [81] Q. Lu, M. Reece, and Z.-Z. Xianyu. “Missing scalars at the cosmological collider.” *JHEP* 12 (2021), p. 098. DOI: [10.1007/JHEP12\(2021\)098](https://doi.org/10.1007/JHEP12(2021)098). arXiv: [2108.11385](https://arxiv.org/abs/2108.11385) [[hep-ph](#)].
- [82] L.-T. Wang, Z.-Z. Xianyu, and Y.-M. Zhong. “Precision calculation of inflation correlators at one loop.” *JHEP* 02 (2022), p. 085. DOI: [10.1007/JHEP02\(2022\)085](https://doi.org/10.1007/JHEP02(2022)085). arXiv: [2109.14635](https://arxiv.org/abs/2109.14635) [[hep-ph](#)].
- [83] L. Pinol et al. “Inflationary flavor oscillations and the cosmic spectroscopy.” (2021). arXiv: [2112.05710](https://arxiv.org/abs/2112.05710) [[hep-th](#)].
- [84] Y. Cui and Z.-Z. Xianyu. “Probing Leptogenesis with the Cosmological Collider.” *Phys. Rev. Lett.* 129.11 (2022), p. 111301. DOI: [10.1103/PhysRevLett.129.111301](https://doi.org/10.1103/PhysRevLett.129.111301). arXiv: [2112.10793](https://arxiv.org/abs/2112.10793) [[hep-ph](#)].
- [85] X. Tong and Z.-Z. Xianyu. “Large spin-2 signals at the cosmological collider.” *JHEP* 10 (2022), p. 194. DOI: [10.1007/JHEP10\(2022\)194](https://doi.org/10.1007/JHEP10(2022)194). arXiv: [2203.06349](https://arxiv.org/abs/2203.06349) [[hep-ph](#)].
- [86] M. Reece, L.-T. Wang, and Z.-Z. Xianyu. “Large-Field Inflation and the Cosmological Collider.” (2022). arXiv: [2204.11869](https://arxiv.org/abs/2204.11869) [[hep-ph](#)].
- [87] X. Chen, R. Ebadi, and S. Kumar. “Classical cosmological collider physics and primordial features.” *JCAP* 08 (2022), p. 083. DOI: [10.1088/1475-7516/2022/08/083](https://doi.org/10.1088/1475-7516/2022/08/083). arXiv: [2205.01107](https://arxiv.org/abs/2205.01107) [[hep-ph](#)].
- [88] Z. Qin and Z.-Z. Xianyu. “Phase information in cosmological collider signals.” *JHEP* 10 (2022), p. 192. DOI: [10.1007/JHEP10\(2022\)192](https://doi.org/10.1007/JHEP10(2022)192). arXiv: [2205.01692](https://arxiv.org/abs/2205.01692) [[hep-th](#)].
- [89] G. Cabass et al. “Parity violation in the scalar trispectrum: no-go theorems and yes-go examples.” (2022). arXiv: [2210.02907](https://arxiv.org/abs/2210.02907) [[hep-th](#)].
- [90] G. Cabass, M. M. Ivanov, and O. H. E. Philcox. “Colliding Ghosts: Constraining Inflation with the Parity-Odd Galaxy Four-Point Function.” (2022). arXiv: [2210.16320](https://arxiv.org/abs/2210.16320) [[astro-ph.CO](#)].

- [91] X. Niu et al. “Gravitational Wave Probes of Massive Gauge Bosons at the Cosmological Collider.” (2022). arXiv: [2211.14331 \[hep-ph\]](#).
- [92] X. Niu et al. “Parity-Odd and Even Trispectrum from Axion Inflation.” (2022). arXiv: [2211.14324 \[hep-ph\]](#).
- [93] S. Aoki. “Continuous spectrum on cosmological collider.” *JCAP* 04 (2023), p. 002. DOI: [10.1088/1475-7516/2023/04/002](#). arXiv: [2301.07920 \[hep-th\]](#).
- [94] D. Werth, L. Pinol, and S. Renaux-Petel. “Cosmological Flow of Primordial Correlators.” (2023). arXiv: [2302.00655 \[hep-th\]](#).
- [95] X. Tong et al. “BCS in the Sky: Signatures of Inflationary Fermion Condensation.” (2023). arXiv: [2304.09428 \[hep-th\]](#).
- [96] S. Jazayeri, S. Renaux-Petel, and D. Werth. “Shapes of the Cosmological Low-Speed Collider.” (2023). arXiv: [2307.01751 \[hep-th\]](#).
- [97] Y. Yin. “The cosmological collider signal in the non-BD initial states.” (2023). arXiv: [2309.05244 \[hep-ph\]](#).
- [98] D. Stefanyshyn, X. Tong, and Y. Zhu. “Cosmological Correlators Through the Looking Glass: Reality, Parity, and Factorisation.” (2023). arXiv: [2309.07769 \[hep-th\]](#).
- [99] P. Chakraborty and J. Stout. “Light Scalars at the Cosmological Collider.” (2023). arXiv: [2310.01494 \[hep-th\]](#).
- [100] L. Pinol, S. Renaux-Petel, and D. Werth. “The Cosmological Flow: A Systematic Approach to Primordial Correlators.” (2023). arXiv: [2312.06559 \[astro-ph.CO\]](#).
- [101] N. Arkani-Hamed et al. “The Cosmological Bootstrap: Inflationary Correlators from Symmetries and Singularities.” *JHEP* 04 (2020), p. 105. DOI: [10.1007/JHEP04\(2020\)105](#). arXiv: [1811.00024 \[hep-th\]](#).
- [102] C. Sleight. “A Mellin Space Approach to Cosmological Correlators.” *JHEP* 01 (2020), p. 090. DOI: [10.1007/JHEP01\(2020\)090](#). arXiv: [1906.12302 \[hep-th\]](#).
- [103] C. Sleight and M. Taronna. “Bootstrapping Inflationary Correlators in Mellin Space.” *JHEP* 02 (2020), p. 098. DOI: [10.1007/JHEP02\(2020\)098](#). arXiv: [1907.01143 \[hep-th\]](#).
- [104] D. Baumann et al. “The cosmological bootstrap: weight-shifting operators and scalar seeds.” *JHEP* 12 (2020), p. 204. DOI: [10.1007/JHEP12\(2020\)204](#). arXiv: [1910.14051 \[hep-th\]](#).
- [105] D. Baumann et al. “The Cosmological Bootstrap: Spinning Correlators from Symmetries and Factorization.” *SciPost Phys.* 11 (2021), p. 071. DOI: [10.21468/SciPostPhys.11.3.071](#). arXiv: [2005.04234 \[hep-th\]](#).
- [106] E. Pajer, D. Stefanyshyn, and J. Supel. “The Boostless Bootstrap: Amplitudes without Lorentz boosts.” *JHEP* 12 (2020). [Erratum: *JHEP* 04, 023 (2022)], p. 198. DOI: [10.1007/JHEP12\(2020\)198](#). arXiv: [2007.00027 \[hep-th\]](#).

- [107] C. Sleight and M. Taronna. “From AdS to dS exchanges: Spectral representation, Mellin amplitudes, and crossing.” *Phys. Rev. D* 104.8 (2021), p. L081902. DOI: [10.1103/PhysRevD.104.L081902](https://doi.org/10.1103/PhysRevD.104.L081902). arXiv: [2007.09993](https://arxiv.org/abs/2007.09993) [hep-th].
- [108] H. Goodhew, S. Jazayeri, and E. Pajer. “The Cosmological Optical Theorem.” *JCAP* 04 (2021), p. 021. DOI: [10.1088/1475-7516/2021/04/021](https://doi.org/10.1088/1475-7516/2021/04/021). arXiv: [2009.02898](https://arxiv.org/abs/2009.02898) [hep-th].
- [109] E. Pajer. “Building a Boostless Bootstrap for the Bispectrum.” *JCAP* 01 (2021), p. 023. DOI: [10.1088/1475-7516/2021/01/023](https://doi.org/10.1088/1475-7516/2021/01/023). arXiv: [2010.12818](https://arxiv.org/abs/2010.12818) [hep-th].
- [110] S. Jazayeri, E. Pajer, and D. Stefanyszyn. “From locality and unitarity to cosmological correlators.” *JHEP* 10 (2021), p. 065. DOI: [10.1007/JHEP10\(2021\)065](https://doi.org/10.1007/JHEP10(2021)065). arXiv: [2103.08649](https://arxiv.org/abs/2103.08649) [hep-th].
- [111] S. Melville and E. Pajer. “Cosmological Cutting Rules.” *JHEP* 05 (2021), p. 249. DOI: [10.1007/JHEP05\(2021\)249](https://doi.org/10.1007/JHEP05(2021)249). arXiv: [2103.09832](https://arxiv.org/abs/2103.09832) [hep-th].
- [112] H. Goodhew et al. “Cutting cosmological correlators.” *JCAP* 08 (2021), p. 003. DOI: [10.1088/1475-7516/2021/08/003](https://doi.org/10.1088/1475-7516/2021/08/003). arXiv: [2104.06587](https://arxiv.org/abs/2104.06587) [hep-th].
- [113] C. Sleight and M. Taronna. “On the consistency of (partially-)massless matter couplings in de Sitter space.” *JHEP* 10 (2021), p. 156. DOI: [10.1007/JHEP10\(2021\)156](https://doi.org/10.1007/JHEP10(2021)156). arXiv: [2106.00366](https://arxiv.org/abs/2106.00366) [hep-th].
- [114] H. Gomez, R. L. Jusinkas, and A. Lipstein. “Cosmological Scattering Equations.” *Phys. Rev. Lett.* 127.25 (2021), p. 251604. DOI: [10.1103/PhysRevLett.127.251604](https://doi.org/10.1103/PhysRevLett.127.251604). arXiv: [2106.11903](https://arxiv.org/abs/2106.11903) [hep-th].
- [115] J. Bonifacio, E. Pajer, and D.-G. Wang. “From amplitudes to contact cosmological correlators.” *JHEP* 10 (2021), p. 001. DOI: [10.1007/JHEP10\(2021\)001](https://doi.org/10.1007/JHEP10(2021)001). arXiv: [2106.15468](https://arxiv.org/abs/2106.15468) [hep-th].
- [116] D. Meltzer. “The inflationary wavefunction from analyticity and factorization.” *JCAP* 12.12 (2021), p. 018. DOI: [10.1088/1475-7516/2021/12/018](https://doi.org/10.1088/1475-7516/2021/12/018). arXiv: [2107.10266](https://arxiv.org/abs/2107.10266) [hep-th].
- [117] M. Hogervorst, J. Penedones, and K. S. Vaziri. “Towards the non-perturbative cosmological bootstrap.” (2021). arXiv: [2107.13871](https://arxiv.org/abs/2107.13871) [hep-th].
- [118] L. Di Pietro, V. Gorbenko, and S. Komatsu. “Analyticity and unitarity for cosmological correlators.” *JHEP* 03 (2022), p. 023. DOI: [10.1007/JHEP03\(2022\)023](https://doi.org/10.1007/JHEP03(2022)023). arXiv: [2108.01695](https://arxiv.org/abs/2108.01695) [hep-th].
- [119] C. Sleight and M. Taronna. “From dS to AdS and back.” *JHEP* 12 (2021), p. 074. DOI: [10.1007/JHEP12\(2021\)074](https://doi.org/10.1007/JHEP12(2021)074). arXiv: [2109.02725](https://arxiv.org/abs/2109.02725) [hep-th].
- [120] G. Cabass et al. “Bootstrapping large graviton non-Gaussianities.” *JHEP* 05 (2022), p. 077. DOI: [10.1007/JHEP05\(2022\)077](https://doi.org/10.1007/JHEP05(2022)077). arXiv: [2109.10189](https://arxiv.org/abs/2109.10189) [hep-th].

- [121] X. Tong, Y. Wang, and Y. Zhu. “Cutting rule for cosmological collider signals: a bulk evolution perspective.” *JHEP* 03 (2022), p. 181. DOI: [10.1007/JHEP03\(2022\)181](https://doi.org/10.1007/JHEP03(2022)181). arXiv: [2112.03448](https://arxiv.org/abs/2112.03448) [[hep-th](#)].
- [122] D. Baumann et al. “Linking the singularities of cosmological correlators.” *JHEP* 09 (2022), p. 010. DOI: [10.1007/JHEP09\(2022\)010](https://doi.org/10.1007/JHEP09(2022)010). arXiv: [2106.05294](https://arxiv.org/abs/2106.05294) [[hep-th](#)].
- [123] H. Gomez, R. Lipinski Jusinskas, and A. Lipstein. “Cosmological scattering equations at tree-level and one-loop.” *JHEP* 07 (2022), p. 004. DOI: [10.1007/JHEP07\(2022\)004](https://doi.org/10.1007/JHEP07(2022)004). arXiv: [2112.12695](https://arxiv.org/abs/2112.12695) [[hep-th](#)].
- [124] D. Baumann et al. “Snowmass White Paper: The Cosmological Bootstrap.” *2022 Snowmass Summer Study*. 2022. arXiv: [2203.08121](https://arxiv.org/abs/2203.08121) [[hep-th](#)].
- [125] T. Heckelbacher et al. “Analytical evaluation of cosmological correlation functions.” *JHEP* 08 (2022), p. 139. DOI: [10.1007/JHEP08\(2022\)139](https://doi.org/10.1007/JHEP08(2022)139). arXiv: [2204.07217](https://arxiv.org/abs/2204.07217) [[hep-th](#)].
- [126] G. L. Pimentel and D.-G. Wang. “Boostless cosmological collider bootstrap.” *JHEP* 10 (2022), p. 177. DOI: [10.1007/JHEP10\(2022\)177](https://doi.org/10.1007/JHEP10(2022)177). arXiv: [2205.00013](https://arxiv.org/abs/2205.00013) [[hep-th](#)].
- [127] S. Jazayeri and S. Renaux-Petel. “Cosmological bootstrap in slow motion.” *JHEP* 12 (2022), p. 137. DOI: [10.1007/JHEP12\(2022\)137](https://doi.org/10.1007/JHEP12(2022)137). arXiv: [2205.10340](https://arxiv.org/abs/2205.10340) [[hep-th](#)].
- [128] Z. Qin and Z.-Z. Xianyu. “Helical Inflation Correlators: Partial Mellin-Barnes and Bootstrap Equations.” (2022). arXiv: [2208.13790](https://arxiv.org/abs/2208.13790) [[hep-th](#)].
- [129] Z.-Z. Xianyu and H. Zhang. “Bootstrapping one-loop inflation correlators with the spectral decomposition.” *JHEP* 04 (2023), p. 103. DOI: [10.1007/JHEP04\(2023\)103](https://doi.org/10.1007/JHEP04(2023)103). arXiv: [2211.03810](https://arxiv.org/abs/2211.03810) [[hep-th](#)].
- [130] D.-G. Wang, G. L. Pimentel, and A. Achúcarro. “Bootstrapping Multi-Field Inflation: non-Gaussianities from light scalars revisited.” (2022). arXiv: [2212.14035](https://arxiv.org/abs/2212.14035) [[astro-ph.CO](#)].
- [131] X. Chen, J. Fan, and L. Li. “New inflationary probes of axion dark matter.” (2023). arXiv: [2303.03406](https://arxiv.org/abs/2303.03406) [[hep-ph](#)].
- [132] Z. Qin and Z.-Z. Xianyu. “Closed-Form Formulae for Inflation Correlators.” (2023). arXiv: [2301.07047](https://arxiv.org/abs/2301.07047) [[hep-th](#)].
- [133] Z. Qin and Z.-Z. Xianyu. “Inflation Correlators at the One-Loop Order: Nonanalyticity, Factorization, Cutting Rule, and OPE.” (2023). arXiv: [2304.13295](https://arxiv.org/abs/2304.13295) [[hep-th](#)].
- [134] Z. Qin and Z.-Z. Xianyu. “Nonanalyticity and On-Shell Factorization of Inflation Correlators at All Loop Orders.” (2023). arXiv: [2308.14802](https://arxiv.org/abs/2308.14802) [[hep-th](#)].
- [135] Z.-Z. Xianyu and J. Zang. “Inflation Correlators with Multiple Massive Exchanges.” (2023). arXiv: [2309.10849](https://arxiv.org/abs/2309.10849) [[hep-th](#)].

- [136] D. Green et al. “Positivity from Cosmological Correlators.” (2023). arXiv: [2310.02490 \[hep-th\]](#).
- [137] C. Duaso Pueyo and E. Pajer. “A Cosmological Bootstrap for Resonant Non-Gaussianity.” (2023). arXiv: [2311.01395 \[hep-th\]](#).
- [138] S. De and A. Pokraka. “Cosmology meets cohomology.” (2023). arXiv: [2308.03753 \[hep-th\]](#).
- [139] S. Albayrak and S. Kharel. “Towards the higher point holographic momentum space amplitudes.” *JHEP* 02 (2019), p. 040. DOI: [10.1007/JHEP02\(2019\)040](#). arXiv: [1810.12459 \[hep-th\]](#).
- [140] S. Albayrak, C. Chowdhury, and S. Kharel. “New relation for Witten diagrams.” *JHEP* 10 (2019), p. 274. DOI: [10.1007/JHEP10\(2019\)274](#). arXiv: [1904.10043 \[hep-th\]](#).
- [141] S. Albayrak and S. Kharel. “Towards the higher point holographic momentum space amplitudes. Part II. Gravitons.” *JHEP* 12 (2019), p. 135. DOI: [10.1007/JHEP12\(2019\)135](#). arXiv: [1908.01835 \[hep-th\]](#).
- [142] S. Albayrak and S. Kharel. “Spinning loop amplitudes in anti-de Sitter space.” *Phys. Rev. D* 103.2 (2021), p. 026004. DOI: [10.1103/PhysRevD.103.026004](#). arXiv: [2006.12540 \[hep-th\]](#).
- [143] S. Albayrak, S. Kharel, and D. Meltzer. “On duality of color and kinematics in (A)dS momentum space.” *JHEP* 03 (2021), p. 249. DOI: [10.1007/JHEP03\(2021\)249](#). arXiv: [2012.10460 \[hep-th\]](#).
- [144] S. Albayrak and S. Kharel. “All plus four point (A)dS graviton function using generalized on-shell recursion relation.” *JHEP* 05 (2023), p. 151. DOI: [10.1007/JHEP05\(2023\)151](#). arXiv: [2302.09089 \[hep-th\]](#).
- [145] Y. Wang. “Inflation, Cosmic Perturbations and Non-Gaussianities.” *Commun. Theor. Phys.* 62 (2014), pp. 109–166. DOI: [10.1088/0253-6102/62/1/19](#). arXiv: [1303.1523 \[hep-th\]](#).
- [146] X. Chen, Y. Wang, and Z.-Z. Xianyu. “Schwinger-Keldysh Diagrammatics for Primordial Perturbations.” *JCAP* 12 (2017), p. 006. DOI: [10.1088/1475-7516/2017/12/006](#). arXiv: [1703.10166 \[hep-th\]](#).
- [147] D. Baumann and L. McAllister. “Inflation and String Theory.” Cambridge Monographs on Mathematical Physics. Cambridge University Press, 2015. DOI: [10.1017/CB09781316105733](#). arXiv: [1404.2601 \[hep-th\]](#).
- [148] K. Deshpande, S. Kumar, and R. Sundrum. “TwInflation.” *JHEP* 21 (2020), p. 147. DOI: [10.1007/JHEP07\(2021\)147](#). arXiv: [2101.06275 \[hep-ph\]](#).

- [149] H. M. Lee and A. G. Menkara. “Pseudo-Nambu-Goldstone inflation with twin waterfalls.” *Phys. Lett. B* 834 (2022), p. 137483. DOI: [10.1016/j.physletb.2022.137483](https://doi.org/10.1016/j.physletb.2022.137483). arXiv: [2206.05523](https://arxiv.org/abs/2206.05523) [[hep-ph](#)].
- [150] H. M. Lee and A. Menkara. “Graceful exit from inflation and reheating with twin waterfalls.” (2023). arXiv: [2304.08686](https://arxiv.org/abs/2304.08686) [[hep-ph](#)].
- [151] X. Chen et al. “Observational signatures and non-Gaussianities of general single field inflation.” *JCAP* 01 (2007), p. 002. DOI: [10.1088/1475-7516/2007/01/002](https://doi.org/10.1088/1475-7516/2007/01/002). arXiv: [hep-th/0605045](https://arxiv.org/abs/hep-th/0605045).